STUDIA UNIVERSITATIS BABEŞ-BOLYAI BIOLOGIA, 70, 1, 2025 (p. 245-286)
doi:10.24193/subbbiol.2025.1.12

Community-level physiological profiling of carbon substrate metabolization by microbial communities associated to sediments and water in karstic caves from Romania

Diana Felicia Panait[1,2,3]✉, Andrei Marian Panait[4], Adorján Cristea[5], Erika Andrea Levei[6], Oana Teodora Moldovan[7], Horia Leonard Banciu[8]✉

1. Institute for Research, Development in Applied Natural Sciences, Babeş-Bolyai University, Cluj-Napoca, Romania; 2. Electron Microscopy Center, Faculty of Biology and Geology, Babeş-Bolyai University, Cluj-Napoca, Romania; 3. Doctoral School of Integrative Biology, Faculty of Biology and Geology, Babeş-Bolyai University, Cluj-Napoca, Romania; 4. S.C. Brillio Romania SRL, Cluj-Napoca, Romania; 5. Department of Ecology and Taxonomy, Faculty of Biology and Geology, Babeş-Bolyai University, Cluj-Napoca, Romania; 6. INCDO-INOE 2000, Research Institute for Analytical Instrumentation, Cluj-Napoca, Romania; 7. Emil Racoviță Institute of Speleology, Cluj-Napoca Department, Cluj-Napoca, Romania; 8. Department of Molecular Biology and Biotechnology, Faculty of Biology and Geology, Babeş-Bolyai University.

✉***Corresponding authors, E-mail:*** *diana.bogdan@ubbcluj.ro, horia.banciu@ubbcluj.ro*

Article history: Received 28 February 2025; Revised 30 April 2025; Accepted 18 May 2025; Available online 25 June 2025

Abstract. Cave ecosystems comprise specialized microbial communities that play essential roles in biogeochemical cycles; yet their metabolic capabilities and ecological functions are not fully understood. As conventional cultivation techniques provide limited insights into the metabolic capabilities, methods based on direct functionality screening may improve our knowledge of cave microbial activity. In this study, the Community-Level Physiological Profiling (CLPP) based on Biolog® EcoPlate™ approach was applied to assess carbon (C) substrate utilization by microbial communities associated with 36 environamental samples collected from five karstic caves (Cloşani, Ferice, Leşu, Muierilor, and Topolniţa) in Romania. Principal Component Analysis (PCA) and Generalized Additive Models (GAMs) statistics were employed to infer the patterns of C substrate metabolization and their environmental drivers. Environmental variables such as sodium (Na) and

electrical conductivity (EC) significantly impacted C substrate utilization capabilities as indicated by both PCA and GAM. The latter analysis elucidated non-linear relationships between variables, such as EC, Na, and Mg, and microbial metabolic diversity indices. However, distinct C substrate utilization patterns were detected among sampled sites and chemical types. Unlike moonmilk samples where associated microbial communities appeared as exhibiting low C substrate utilization, the highest activity was shown in cave pool water samples with the associated microbial communities extensively consuming D-galacturonic acid and Tween 80. Conversely, substrates like L-threonine and α-ketobutyric acid showed limited utilization across all cave samples. Average Well Color Development (AWCD) and Shannon diversity indices indicated that microbial communities associated to samples from Cloșani and Muierilor caves demonstrated the highest metabolic diversity. Our findings suggested that metabolic profiling using Biolog® EcoPlate™ method combined with multivariate statistical methods might prove a suitable analysis approach to effectively screen for cave microbial functionality and the probable environmental drivers. Besides, this work distinguishes from similar studies by relying on GAM analysis to predict the environmental factors governing the microbially-mediated organic carbon degradation in subterranean ecosystems.

Keywords: caves, community-level physiological profile, generalized additive models, microbial communities, organic carbon substrates.

Introduction

The nutrient-limited subterranean ecosystems are inhabited by microorganisms with slow metabolism and growth rates (Epure *et al*., 2014). These cave-dwelling microbes are assumedly involved in biogeochemical cycles of major elements such as C, N, P or S. Therefore, investigation of taxonomic and metabolic diversity is crucial in enlarging our understanding of the interactions and ecological roles of cave microorganisms (Barton and Northup., 2007). Yet, investigating the microbial taxonomic and functional diversity in cave ecosystems poses significant challenges, including the limitations of the traditional culturing techniques, which recover only a small fraction of the members of microbial communities (Jones *et al*., 2015). Additionally, culture-dependent techniques provide limited understanding of microbial activity *in situ*, failing to capture the complexity of functional relationships within microbial communities. Therefore, complementary rapid and effective methods to directly assess the metabolic

potential of cave microbial communities are beneficial. For example, the Community-Level Physiological Profiles (CLPP) using EcoPlate™ plates (Biolog® Inc., Hayward, CA, USA) approach may be useful in characterizing the community functionality, offering a clearer view of microbial functional diversity and ecological potential in cave environment. The Biolog® EcoPlate™ is a time- and cost-effective tool that has been used to monitor the spatio-temporal carbon substrate preferences of microbial communities inhabiting a diverse range of habitats including groundwater (Melita *et al*., 2023), surface freshwater (Boteva *et al*., 2024), brackish-to-saline waters (Cristea *et al*., 2014), wetlands (Teng *et al*., 2020), agricultural soils (Rutgers et al., 2015), rhizosphere (Cacchio and Del Gallo, 2019), volcanic soils and mud (Amaresan *et al*., 2018; Asif *et al*., 2024), and limestone monuments (Andrei *et al*., 2017). Moreover, this versatile approach has been applied to assess the carbon utilization by bacterial communities in karst caves (Yun *et al*., 2018) and lava tube ice caves (O'Connor *et al*., 2021). Overall, the noteworthy benefit of this method is that it is comparable to high-resolution, yet more resource-consuming molecular techniques such as metagenomics. Although the Biolog® EcoPlate™ method provides a limited information on microbial metabolic capabilities, its rapidity in profiling the community-wide metabolic activity makes it a valuable complementary tool for metabolic fingerprinting with potential to enhance our understanding of functional diversity within cave ecosystems.

Despite the increasing interest in exploring cave microbial communities, considerable gaps remain in understanding both individual and community-driven microbial metabolic processes in caves. Present limitations result from focusing on taxonomy rather than functionality, scarcity of in situ studies, metabolite profiling, and a poor understanding of biogeochemical processes in caves or other subterranean environments. Here, we aimed to employ the Biolog® EcoPlate™ tool to survey the carbon substrate utilization patterns of microbial communities inhabiting cave pool water, water sediment (limon), dry sediments, and moonmilk (white precipitate with aggregates of fine carbonate crystals) from five Romanian caves, thereby addressing the diversity of carbon metabolization traits and the delineation of their main environmental drivers.

Materials and methods

Sampling sites

Five karstic caves (Cloşani, Ferice, Leşu, Muierilor, and Topolniţa) were sampled in this study (Figure 1). A brief description of sampled caves is provided below.

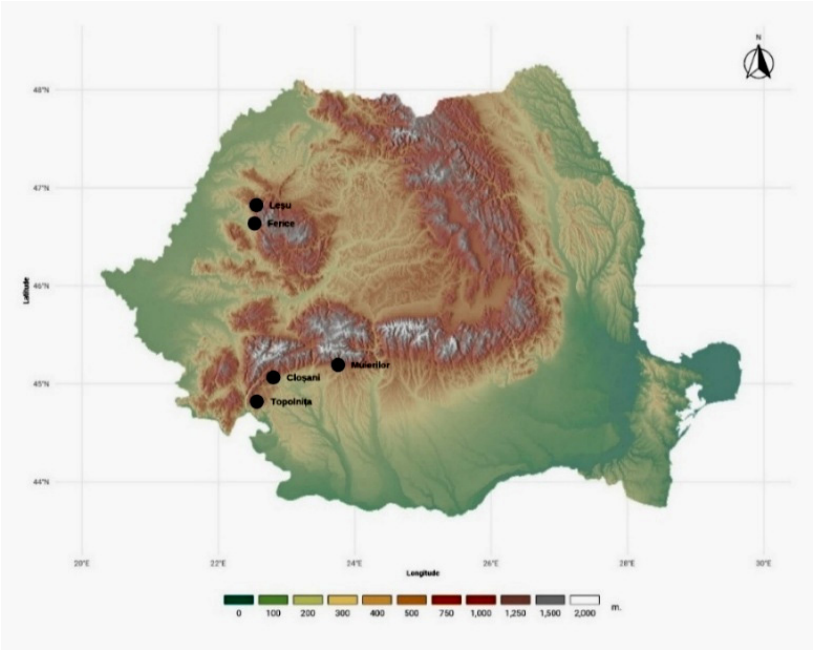

Figure 1. Geographic and altitudinal distribution of the sampled karstic Romanian caves. The map was generated using R Studio with topographic data using the 'geodata' package with the data source from Shuttle Radar Topography Mission (SRTM), specifically the hole-filled CGIAR-SRTM (90 m resolution) from https://srtm.csi.cgiar.org/.

Cloșani Cave is located in Southern Carpathians (near Cloșani village). It has a narrow entrance found at an altitude of 443 m above sea level (a.s.l). The two galleries have a length of 1100 m, and temperatures of about 11°C in the depth of the cave, increased humidity and a lack of air currents (Bleahu *et al*., 1976).

Ferice Cave is located in North-Western Romania, Apuseni Mountains at an elevation of 410 m a.s.l. in a region with oceanic climate influences. A low-flow stream crosses the main horizontal passage, which measures around 260 meters in length. During the winter season a small number of bats frequent the cave. The temperature within the cave ranges from 11.4°C to 12.7°C and the humidity from 80% (lowest value during May) to 95% (November) (Moldovan *et al*., 2023).

Leşu Cave (Peştera cu Apă din Valea Leşului) is situated in the Apuseni Mountains and designated protected area classified as a natural reserve (type IV IUCN). The Leşu cave system features a primary gallery approximately 1 km long, traversed by a meandering water stream for the initial 300 m, forming

alluvial terraces. The annual air temperature within the cave averages between 8.5° and 10°C. The cave has a significant hibernation colony of multiple bat species, primarily near the entrance (Zoltan and Szántó, 2003; Bücs *et al*., 2012).

Muierilor Cave is located in the Southern Carpathians near Baia de Fier, Gorj County, at approximately 645 m a.s.l. Its karstic system has multiple chambers and a total length of over 8000 m. The cave system includes pristine sections and a show cave (Level 2 – accessible for visitors). It is a protected natural monument with designated scientific reserves (Mirea *et al*., 2021).

Topolniţa Cave is located in the Southern Carpathians, at an elevation of ~400 m a.s.l. It is distinguishable by its extensive karst system covering more than 20 km^2 and by significant bat colonies that produce large guano deposits (Cleary *et al*., 2019; Moldovan *et al*., 2023).

Sample collection and Biolog® EcoPlate™ assay

Environmental samples were collected from the studied cave sites, including cave water and substrate (limon), dry sediment, and moonmilk (Table 1). Pool substrate samples (limon) were further considered and processed as 'sediment' samples. All samples were collected from areas free from human impact, including samples from show caves like Muierilor. Five grams of fresh sediment (including limon and moonmilk samples) were suspended in 50 mL NaCl 0.85% solution and stirred for about 30 minutes on a water-bath shaker (150-200 rpm) at 23°C. After one hour of on-the-table sedimentation, 100 µL of the resulted cellular suspension was inoculated in each well from the EcoPlate™ plates (Biolog® Inc., Hayward, CA, USA) under a laminar airflow hood, ensuring the prevention of contamination throughout all procedures. The 96-well Biolog® EcoPlate™ contains a total of 31 carbon substrates in triplicate and three wells without substrate serving as a control. One plate was used for each sample. No additional biological or technical replicates were included beyond the plate's built-in triplicates.

The optical density measurements at 590 nm (OD590) were performed on a plate reader (FLUOstar® Omega, BMG Labtech, Offenburg, Germany). Plates were incubated up to 8 days (200 hours) at 16 °C (chosen as near-environmental value) and specific intervals of time between readings were established based on the literature review which mostly depends on the color development on plates (Garland, 1997; Iţcuş *et al*., 2016). A 12-hour interval between measurements was established and carried out until no changes in both color development and OD_{590} values were detected. Variability in microbial inoculum size, inherent to environmental samples, may contribute to the observed differences in metabolic profiles.

Table 1. Summary of the sampled caves and sample types used in this study.

Sample nr.	Cave	Sample ID	Sample type
1	Cloşani	PCDF2-APA	water
2		PCDF3-APA	water
3		LAB1	sediment
4		LAB2	sediment
5		LAB3	sediment
6		GHICA1	sediment
7		GHICA2	sediment
8		GHICA3	sediment
9		PCDF1	sediment
10		PCDF2-LIMON	limon (sediment)
11		PCDF3-LIMON	limon (sediment)
12	Ferice	PFDF1	sediment
13		PFDF2	sediment
14		PFDF3	sediment
15		PFDF4-SOL	sediment
16		PFDF2MM	moonmilk
17		PFDFMMC	moonmilk
18		PFDF4-APA	water
19		PFDF4-LIMON	limon (sediment)
20	Muierilor	PMDF9-APA	water
21		PMDF10-APA	water
22		PMDF2	sediment
23		PMDF5	sediment
24		PMDF11	sediment
25		PMDF5A	sediment
26	Leşu	PLDF1	sediment
27		PLDF1A	sediment
28		PLDF1B	sediment
29		PLDF4	sediment
30		PLDF2	sediment
31		PLDF1B-APA	water
32		PLDF2-APA	water
33		PLDF3-APA	water
34	Topolniţa	PTDF1	sediment
35		PTDF2	sediment
36		PTDF3	sediment

Physico-chemical analyses

The pH and electrical conductivity (EC) were assessed in water samples and 1/5 sediment-to-water extracts using the Seven Excellence multiparameter (Mettler Toledo, Greifensee, Switzerland). To measure the concentration of elements, one gram of dried sediment was digested with aqua regia (21 mL of 12 M HCl and 7 mL of 15.8 M HNO_3), subsequently filtered and diluted to 100 mL with 0.5 M HNO_3. The *aqua regia*-extractable fraction includes both physiologically available and unavailable metals. Water samples were acidified with 15.8 M HNO_3 and filtered using cellulose acetate membrane filters with a pore size of 0.45 μm for the determination of dissolved metals and phosphorus contents. The concentrations of Na, Mg, K, Ca, and P in water, as well as Na, Mg, K, Ca, P, Al, Fe, S, and Mn in sediments, limon and moomilk were quantified using inductively coupled plasma optical emission spectrometry with an Optima 5300DV (Perkin Elmer, Waltham, MA, USA) spectrometer. Additionally, the concentrations of Al, Fe, As, Cr, Mn, Co, Ni, Cu, and Zn in water, along with As, Cr, Co, Ni, Cu, and Zn in sediments, were determined via inductively coupled mass spectrometry utilizing an Elan DRC II (Perkin Elmer, Waltham, MA, USA). The carbon, and nitrogen contents in sediments were quantified using a Flash 2000 CHNS/O analyzer (ThermoFisher Scientific, Waltham, MA, USA). Total nitrogen (TN) in water was quantified using catalytic combustion, followed by the oxidation of nitrogen monoxide to nitrogen dioxide using ozone, and subsequent detection via chemiluminescence with a Multi N/C 2100S Analyser (Analytik Jena, Jena, Germany). Dissolved carbon (DC) and dissolved inorganic carbon (DIC) were measured in water samples filtered via 0.45 μm PTFE syringe filters using catalytic combustion and infrared detection of CO2 utilizing a Multi N/C 2100S Analyser (Analytik Jena, Jena, Germany). Dissolved organic carbon (DOC) was derived by subtracting dissolved inorganic carbon (DIC) from total carbon (DC). Sulfate (SO_4^{2-}), nitrate (NO^{3-}), chloride (Cl^-), and phosphate (PO_4^{3-}) were quantified using ion chromatography on a 761 Compact IC (Metrohm, Switzerland).

Data acquisition, preprocessing and processing

Data from OD_{590} measurements were extracted from individual .xlsx files using **readxl** package. Data from some samples from Lesu Cave described in Bogdan *et al.* (2023) were reanalyzed in a comparative context and with a more comprehensive statistical analysis. Each sample was identified by its unique sampling site, sample type and the hour of incubation. The absorbance (OD_{590}) values were corrected against water blanks using designated wells and averaged across triplicate measurements for each carbon substrate. Further, the dataset

was processed to remove negative values after correction. Some samples were read up to 360 hours, but given that no changes were detected in the color development or OD_{590} measurements we excluded the timepoints after 204 hours. All analyses were performed using R (R Core Team, 2020) and key packages included the following: readxl version 1.4.3, dplyr version 1.1.4 and tidyr version 1.3.1 for data processing; mgcy version 1.9-1 for GAMs; factoextra version 1.0.7 for PCA; ggplot2 version 3.5.1 and pheatmap version 1.0.12 for data visualization.

Calculation of microbial metabolic diversity metrics

Microbial metabolic diversity metrics were calculated for each sample based on the formulas and indices from the literature (Zak *et al.*, 1994; Feigl *et al.*, 2017) (Table 2). The principal microbial metabolic diversity metrics provide insights into both the metabolic capacity and functional evenness of the microbial communities.

Table 2. Microbial metabolic diversity indices and equations used for calculations

Index	Equations	Definition
Average Well Color Development (AWCD)	AWCD= $\Sigma\frac{C-R}{N}$, C-OD_{590} values of each well R-OD_{590} values of the control well N-number of substrates (31)	Calculated by the differences between the OD_{590} of the wells containing individual carbon sources and the control wells
Richness	-	Represents the number of substrates utilized, defined as those with an absorbance greater than 0.25
Shannon diversity (H index)	$H = -\sum p_i \, log(p_i)$ pi-proportion of each substrate's utilization	Quantifies the diversity of microbial communities by considering both the richness and the proportional utilization of carbon substrates; higher values of H indicate greater diversity, as more substrates are being used more evenly across the microbial community.
Shannon evenness (E)	E=H/log (R) R – substrate richness	Measures how evenly the carbon substrates are utilized by the microbial community, and is derived by dividing the Shannon diversity (H) by the logarithm of substrate richness (R); values close to 1 indicate a more uniform distribution of substrate utilization, while values closer to 0 suggest that a few substrates dominate the activity.

Statistical analyses

Generalized Additive Models (GAMs)

Generalized Additive Models (Simpson, 2024) were employed to explore the link between microbial metabolic diversity metrics and geochemical factors. GAMs allow for non-linear relationships between predictor variables (e.g. values of geochemical or physico-chemical parameters) and response variables (e.g. microbial metrics). These models were fitted using the mgcy package, which applies smooth functions to each predictor. The microbial metrics, including richness, Shannon diversity, and Shannon evenness, were modeled as response variables with smooth terms for key geochemical predictors: pH, EC, and the concentrations of N, C, Na, Mg, K, Ca, P (Equation 1).

Equation 1. The formula for the GAMs which was applies smooth functions to each predictor.

$$Y = \beta_0 + s(pH) + s(EC) + s(N) + s(C) + s(Na) + \cdots + \epsilon$$

Where:

- Y is the microbial metric (Richness, Shannon Diversity, or Evenness),
- s(·) denotes a smooth function applied to each geochemical predictor.

These models allowed us to capture non-linear effects and interactions between environmental conditions and microbial diversity. Moreover, the GAMs were visually inspected for their goodness of fit using residual diagnostics. Model checks and plots of the smooth functions for each predictor were generated to assess the relationship between diversity and geochemical factors.

Principal Component Analysis (PCA)

The Principal Component Analysis (PCA) was used to investigate the joint variation in microbial community metabolic metrics and environmental geochemistry, by reducing the dimensionality of the dataset by identifying the principal components (PCs) that capture most of the variation in the datasets. Particularly, this is a powerful tool for identifying correlations between microbial metabolism (community-physiological profiles) and geochemical properties. In this case, PCA was applied to the combined dataset of microbial metrics such as AWCD, richness, Shannon diversity, Shannon evenness and physico-chemical variables (pH, EC, N, C, Na, Mg, K, Ca, P) using the factoextra package. These variables were scaled to ensure the comparability between measurements with different units for which the relationship between the principal components and

the original standardized variables was established with the equation presented below (Equation 2), in which, Z represents the matrix of principal components, W is the weight matrix that defines the linear combination of the original variables, and X denotes the matrix of original standardized variables which includes microbial metrics and chemical parameters.

Equation 2. The formula used to reduce the dimensionality of the dataset while capturing the most significant variance, facilitating the interpretation of underlying patterns in microbial and chemical interactions.

$$Z = W \times X,$$

Biplots were created to visualize the relationship between microbial metrics and geochemical factors, displaying the sample clustering and contribution of variables.

Data visualization

Boxplots and line plots were used for the representation of microbial activity (AWCD and diversity metrics) across sample types and time points. Heatmaps coupled with hierarchical clustering were created to display metabolic activity patterns across carbon sources, samples and hours. The PCA biplot was used to explore the relationship between microbial metrics and geochemical factors. At the same time, the results of the GAMs depict the non-linear trend between chemistry and microbial diversity.

Results

Physico-chemical characteristics of cave water and sediment samples

Physico-chemical parameters, including pH, EC and the concentration of major elements (N, C, Na, Mg, K, Ca, P) were measured from sediment (limon and moonmilk included here) and water samples, with total nitrogen (TN) and total carbon (TC) considered for N, and C respectively (Table 3). Sediments show high calcium (Ca) concentrations, particularly in LAB3 (454,682 mg/kg) and LAB2 (226,206 mg/kg), reflecting the limestone-rich environment. The phosphorus (P) levels were highly variable, with some sediments, such as PMDF11 (41167 mg/kg) showing higher concentrations compared to PFDF2MM (104 mg/kg). On the other hand, in water samples, the electrical conductivity (EC) was notably higher, specifically PFDF4-APA showing the highest value (359 µS/cm). Overall, the pH of all the samples was basic with variations from 7.8 in sediment sample GHICA2 to

9.3 in LAB1 (sediment) and PFDFMMC (moonmilk). Carbon concentrations varied widely in sediments, ranging from < 100 mg/kg (e.g., PTDF1, LAB1) to 98,400 mg/kg (PMDF2), highlighting localized carbon hotspots. In water, concentrations were more consistent, ranging from 17.3 mg/L to 50.0 mg/L, reflecting its role in transporting dissolved carbon species. Sediments consistently exhibited higher concentrations of elements compared to water, indicating their function as nutrient and mineral reservoirs. The geochemical data were merged with the microbial metabolic diversity metrics by sample ID, allowing for a combined analysis of microbial community structure and environmental chemistry. However, certain elements (Al, Fe, S, Mn, As, Cr, Co, Ni, Cu, Zn) and water-specific parameters (TN, DC, DIC, DOC, SO_4^{2-}, NO_3^-, Cl^-, PO_4^{3-}) were excluded from the PCA due to either their low concentrations or the inability to integrate both sediment and water sample data in the same PCA. Nevertheless, aluminum (Al) and iron (Fe) dominated the sediment samples, with maximum concentrations of 63,089 mg/kg and 55,572 mg/kg, respectively. At the same time, sulfur (S) and trace metals like copper (Cu) and zinc (Zn) showed localized enrichment. In contrast, water samples exhibited significantly lower and more uniform concentrations, with aluminum peaking at 7.84 μg/L and sulfate reaching 48.6 mg/L, reflecting dilution effects and contrasting physico-chemical attributes between sediments and water (Table S2).

Patterns of carbon source utilization in cave samples

The carbon substrate metabolization patterns significantly varied across all assayed cave samples (Figure 2). A higher OD_{590} was recorded for the samples inoculated in the wells containing Tween 40, putrescine and D-xylose, indicating a higher rate of microbial activity toward degradation of these compounds. Conversely, lower OD_{590} values after substrate consumption were exhibited in the wells containing 2-hydroxy benzoic acid and L-threonine suggesting limited microbial capacity to metabolize these compounds. The compounds such as pyruvic acid methyl ester and D-galacturonic acid were overall metabolized in most samples, though with considerable variation in OD values, suggesting functional redundancy in the community.

The average OD for selected carbon substrates indicated that the microbial community from the water samples exhibited the highest metabolic activity for a wide range of carbon sources (Table 4). D-galacturonic acid (mean OD_{590} = 1.22 ± 0.75), D-mannitol (1.05 ± 0.85), N-acetyl-D-glucosamine (1.03 ± 0.72), and Tween 80 (1.03 ± 0.79). In contrast, the microbial communities associated to the moonmilk samples showed the lowest ability to utilize organic C-substrates, with OD_{590} values remaining below 0.5 for most carbon sources.

Table 3. Physico-chemical parameters measured in cave sediment (including limon and moonmilk) and water samples. Total nitrogen (TN) was considered as N, and total carbon (TC) as C, for water samples.

Sample ID	pH	EC	N	C	Na	Mg	K	Ca	P
Sediments									
		µS/cm	mg/kg	mg/kg	mg/kg	mg/kg	mg/kg	mg/kg	mg/kg
PMDF2	8.80	69.0	< 100	98359	79	2833	1336	322967	4843
PMDF5	8.40	73.6	3500	18700	65	1123	2918	29137	9803
PMDF11	8.40	120.5	3180	19086	452	1850	3321	194933	41167
PMDF5A	8.59	102	2452.31	29280	182	6386	2395	112533	14963
PTDF1	8.50	49.7	< 100	417	161	6590	3407	11583	1135
PTDF2	8.80	57.6	< 100	< 100	125	6383	3298	10997	293
PTDF3	8.98	110.7	< 100	16636	170	6820	1806	113666	2022
LAB1	9.30	64.8	< 100	< 100	380	13578	3676	189052	739
LAB2	8.50	112.3	< 100	76500	235	1406	2209	226206	420
LAB3	8.60	104.6	< 100	85700	201	1313	3634	454682	346
GHICA1	8.00	73.9	< 100	1000	444	1810	5557	13265	276
GHICA2	7.80	160.2	< 100	3800	466	1809	5609	16741	501
GHICA3	8.10	89.9	1200	19900	441	1817	5202	65313	498
PCDF1	8.20	40.9	< 100	< 100	111	5873	3433	10023	9990
PFDF1	8.72	77.4	7839	9810	95	17307	5437	31733	879
PFDF2	8.62	69.3	7012	< 100	119	13847	6863	9400	1267
PFDF3	8.34	121.6	7300	3500	157	50533	4653	31757	7107
PFDFMMC	9.30	67.2	2800	97600	329	78570	921	150947	451
PFDF2MM	9.20	58.9	1600	121000	188	85871	518	211096	104
PLDF1	8.67	53.4	2686	37876	60	32210	1248	63833	1367
PLDF1A	8.60	83.9	5550	50429	123	5134	2192	110933	4247
PLDF1B	8.48	80.1	5339	17015	73	2950	2992	60733	1870
PLDF4	8.58	83.5	3079	11243	62	2143	1851	49667	3380
PLDF2	8.12	114.5	6584	34213	125	4297	1982	69000	8930
Water									
		µS/cm	mg/L	mg/L	mg/L	mg/L	mg/L	mg/L	mg/L
PMDF9-APA	8.20	287.5	15.1	18.0	1.625	1.346	5.734	55.90	0.31
PMDF10-APA	8.60	353.3	17.7	19.9	1.686	2.305	8.213	69.72	0.453
PCDF2-APA	8.10	168.4	<0.7	17.3	0.585	2.151	1.036	69.17	48.88
PCDF3-APA	7.90	189.4	<0.7	19.2	0.515	0.742	0.225	45.40	0.17
PFDF4-APA	8.30	359.2	<0.7	50.0	0.642	24.12	0.389	43.64	0.016
PLDF1B-APA	8.10	147.5	0.94	19.1	0.572	0.476	0.398	35.41	0.014
PLDF2-APA	8.10	171.3	0.86	22.2	0.487	0.451	0.373	40.64	0.032
PLDF3-APA	7.90	209.2	<0.7	26.4	0.493	0.873	0.483	48.97	0.004

Table 4. Average OD_{590} (± standard deviation) for selected carbon sources measured using the Biolog® EcoPlate™ method in water and sediment cave sample.

Carbon Source	Water (Mean ± SD)	Sediment (Mean ± SD)	Moonmilk (Mean ± SD)
D-mannitol	1.05 ± 0.85	0.63 ± 0.82	0.05 ± 0.03
N-acetyl-D-glucosamine	1.03 ± 0.72	0.42 ± 0.60	0.02 ± 0.01
L-serine	0.80 ± 0.68	0.55 ± 0.68	0.00 ± 0.00
Tween 80	1.03 ± 0.79	0.49 ± 0.60	0.20 ± 0.24
D-galacturonic acid	1.22 ± 0.75	0.60 ± 0.63	0.13 ± 0.13

Further on, the temporal dynamics based on median absorbance values for the carbon source utilization was assessed across the sample types (Figure 2). An overall higher C substrate utilization compared to the other samples was noted in water samples, specifically for substrates such as D-galacturonic acid, pyruvic acid methyl ester, Tween 40 and N-acetyl-D-glucosamine (Table 4). Certain C-sources, like putrescine and L-arginine, represent substrates for bacterial enzymatic activity, indicating similar patterns in sediment and water, but with generally higher utilization by water-associated communities. The moonmilk microbial communities overall show the lowest C-substrate utilization with many substrates exhibiting little to no increase in absorbance over time (e.g., γ-amino butyric acid, β-methyl-D-glucoside, D-cellobiose), except for D-xylose and 2-hydroxy benzoic acid which depict a higher median absorbance compared to sediment and water samples.

Similarly, the differences in temporal dynamics of median absorbances across the carbon substrates were assessed between sampling sites. The samples from Muierilor Cave showed the highest microbial-driven C-substrate utilization with preference for D-galacturonic acid, L-serine, D-malic acid, L-asparagine, and D-mannitol, suggesting that the communities from this sampling site can utilize a wide variety of substrates. On the other hand, the microbial communities associated to samples from Topolniţa Cave generally show the lowest activity, except for 2-hydroxy benzoic acid. To illustrate differences between samples and the metabolic capabilities of their microbial communities, separate graphs were generated for each sample type (Figures S2–S4). For example, microbial communities in Cloşani water samples exhibit notably high OD values over 1, for 19 carbon sources (Figure S2), suggesting that Cloşani water is the most metabolically active among the water samples. In contrast, the utilization of organic C sources by the microbial communities associated to the Muierilor Cave water samples has a lower activity (OD_{590} values < 0.5) with a few exceptions for substrates like 2-hydroxy benzoic acid, D-malic acid,

D-xylose, L-arginine, L-asparagine, Tween 40 and Tween 80. The sediment samples (Figure S3) show almost similar activity in samples from Leşu and Muierilor caves, yet higher in Leşu, whereas Cloşani, Ferice and Topolniţa caves depict approximately similar lower activity except for 2-hydroxy benzoic acid (Topolniţa), α-keto-butyric Acid (Cloşani) and L-serine (Ferice). In the moonmilk samples from a single sampling point (Ferice; Figure S4), median absorbance indicates that Tween 80 was the most rapidly consumed substrate, followed by Tween 40 and L-phenylalanine.

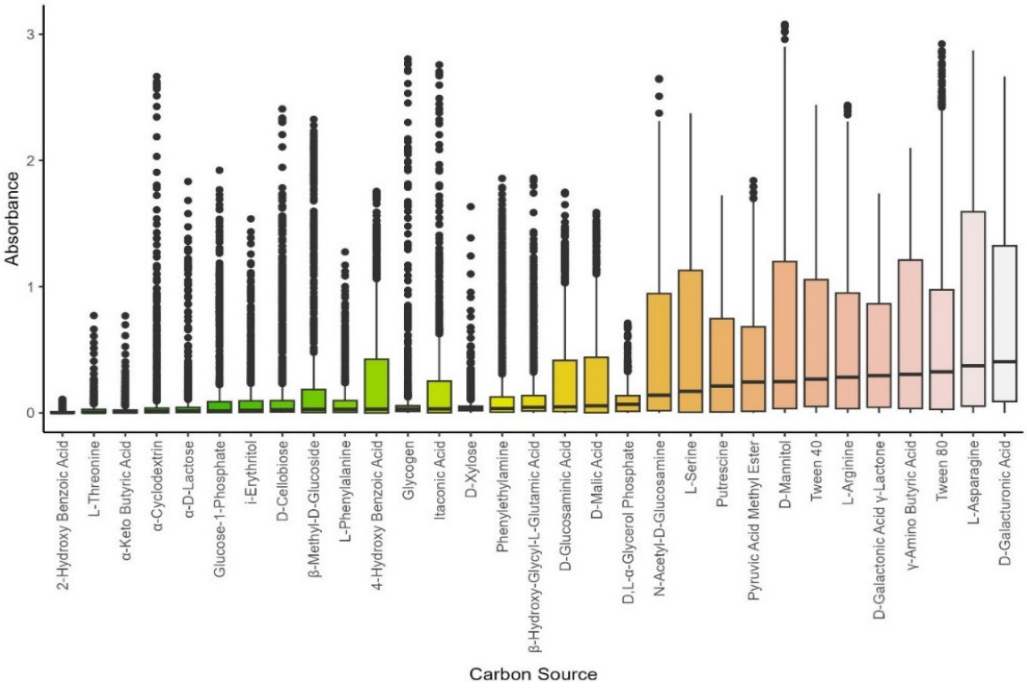

Figure 2. Box plot showing the median absorbance for the metabolization of 31 carbon substrates by microbial communities, highlighting differences in organic carbon substrate utilization and associated metabolic activity. Each box represents the interquartile range (IQR), with whiskers extending to 1.5 times the IQR, and individual dots showing outlier data points. The color coding differentiates the substrates but does not carry a specific meaning.

Estimation of overall carbon metabolization by Average-Well Color Development (AWCD)

The average-well color development (AWCD) at each sampling point for 200 hours provides information on the rates of organic carbon substrate consumption, thus insights into the overall metabolic activity. The overall trend across all sampling locations showed increased substrate utilization after 50 hours of incubation, with site-specific differences in utilization rates. Samples from Muierilor Cave exhibited the fastest changes and highest AWCD values, followed by those from Leșu, Cloșani, Ferice, and Topolnița caves (Figure 3).

The overall substrate metabolization patterns among the three different cave sample types (water, sediment, and moonmilk) were also investigated by the AWCD parameter (Figure 4 and Table S1).

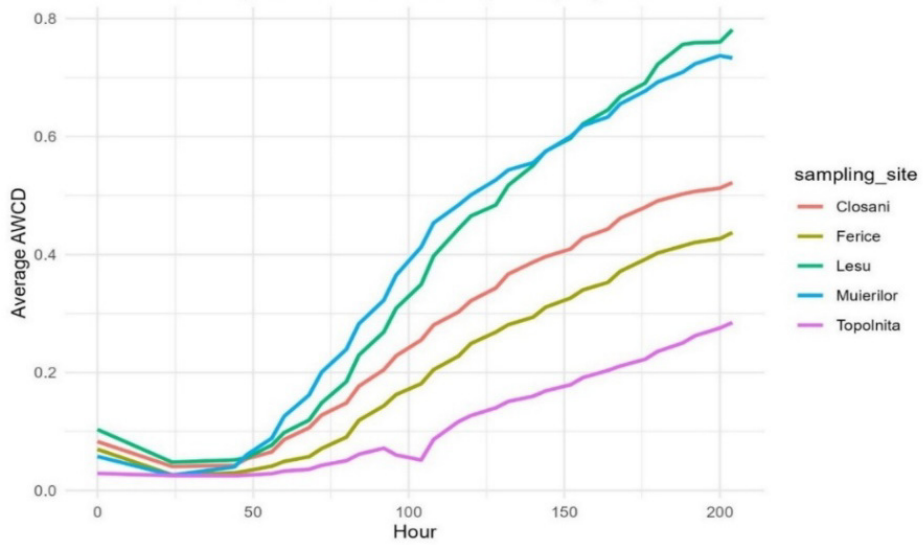

Figure 3. Average-well color development (AWCD) over time for all samples across five sampling sites: Closani, Ferice, Lesu, Muierilor, and Topolnița.

Water samples displayed the highest C-substrate utilizing activity, with a sharp increase in AWCD after 50 hours, reaching a final value of 0.8. The AWCD measured in sediment samples showed moderate, steady increase, reaching approximately 0.5 by the end of the incubation. Moonmilk samples exhibited the lowest AWCD, with a minimal and gradual increase. The overall AWCD patterns across the sample types might reflect significant differences in microbially-mediated organic substrate utilization across these distinct cave niches.

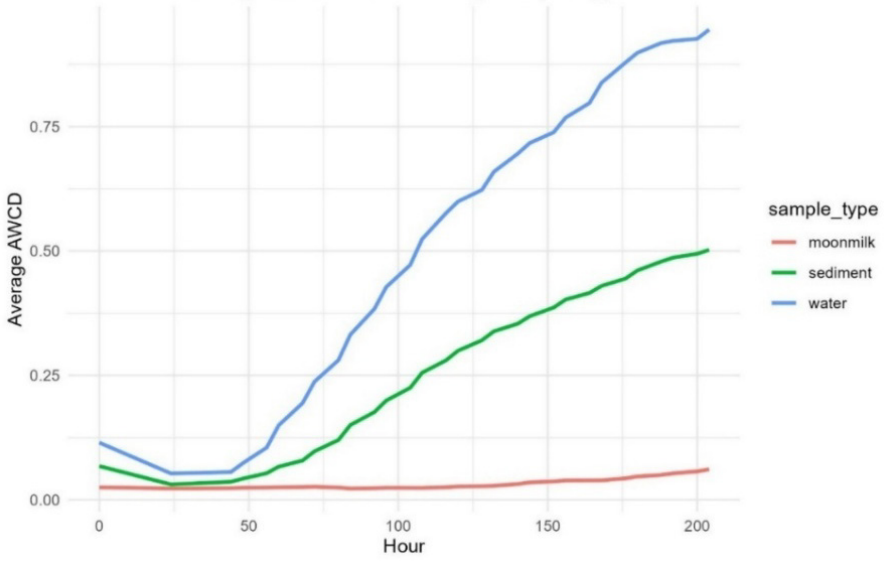

Figure 4. Average-well color development (AWCD) over time measured for the three cave sample types (water, sediment, and moonmilk).

Microbial metabolic diversity metrics across cave samples

Temporal dynamics of metabolic richness and diversity

Shannon diversity metrics were used to assess microbial metabolic diversity for each sampling location (Figure 5) and sample type (Figure S3), whereas maximum richness and H index by sample type were also calculated (Table 5). The Cloşani cave samples showed the highest median values of Shannon diversity metrics (2.83) among all sampled caves (Figure 5), which might indicate that both water and sediment samples likely support the most metabolically diverse microbial communities among tested caves. When comparing sample types, the water samples showed the highest median values of diversity indices (2.9), indicating that the cave aquatic communities are likely more metabolically diverse (i.e. with a broad C-substrate preference) than their sediment or moonmilk counterparts that exhibited lower median values of metabolic diversity indices of 2.75 (sediments), and 2.67 (moonmilk) (Figure S3).

Noteworthy, the moonmilk samples collected from Ferice Cave had the lowest calculated indices (Table S1 and Figure S3), possibly due to a more specialized or less diverse community. The samples from Leşu and Muierilor caves showed moderate metabolic diversity metrics with a median value for Shannon diversity of 2.81 (Leşu) and 2.82 (Muierilor) (Figure 5) with a higher

C-substrate metabolization diversity in sediments compared to water (Table S1). The lowest Shannon diversity values (~2.6) was calculated for samples collected from Topolnița (2.66) and Ferice (2.61) caves. Overall, these findings revealed that metabolic diversity toward organic carbon substrate use differed significantly among sampling locations and sample types, with Cloșani cave samples and water-associated communities, respectively, exhibiting the greatest metabolic diversity.

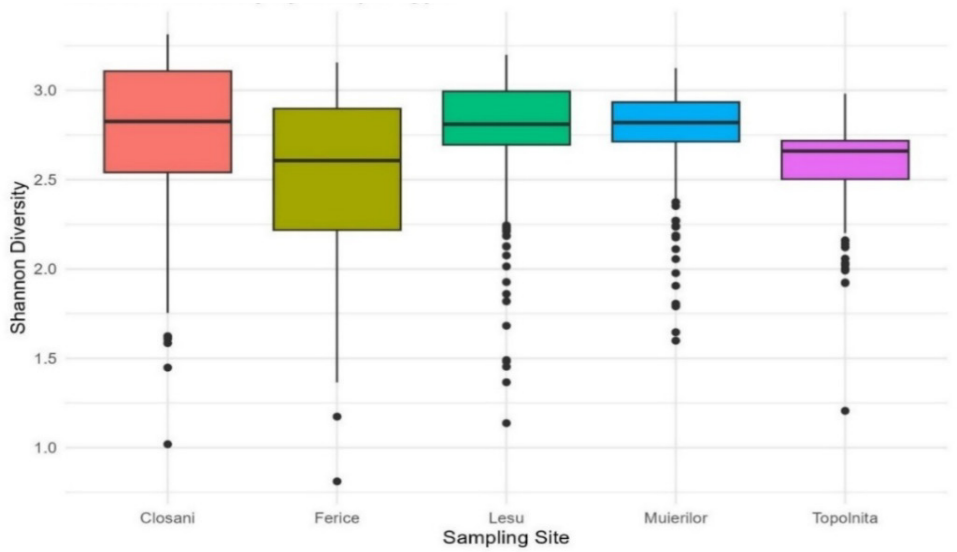

Figure 5. Box plot of Shannon diversity indices based on substrate utilization patterns for microbial communities across sampling sites (Cloșani, Ferice, Lesu, Muierilor, and Topolnița caves). The box colors correspond to different sampling sites, while the black dots represent outliers in Shannon diversity values.

Table 5. Maximum richness and Shannon diversity index by sample type across sampling sites. Richness represents the total number of substrates metabolized, while the Shannon diversity index reflects both the richness and evenness of substrate utilization.

Sample location	Max Richness (Water)	Max Richness (Sediment)	Max Richness (Moonmilk)	Shannon Diversity (Water)	Shannon Diversity (Sediment)	Shannon Diversity (Moonmilk)
Closani	54	76	-	6.45	26.98	-
Ferice	24	78	4	3.16	14.28	6.13
Lesu	56	101	-	8.64	14.94	-
Muierilor	49	62	-	6.19	11.84	-
Topolnita	-	29	-	-	8.62	-

Correlation of the AWCD and richness values

To illustrate both temporal dynamics of C-substrate utilization and diversity of substrate utilization a scatter plot combining AWCD and richness values associated with each sampling site and sample type was generated (Figure 6). The observed values and ranges are reported to illustrate variability across sampling sites and sample types than measures of central tendency (mean or median). Despite some site-specific variations, AWCD was positively correlated with richness (Figure 6). The results indicated that Cloșani Cave may support communities with greater metabolic versatility and a broader diversity of consumed substrates than the other cave sites. Richness values converged at lower AWCD values (0.0-0.5), suggesting baseline diversity despite limited activity. For AWCD values between 0.5 – 1.0, richness increased more consistently among sites (e.g., Leșu, Muierilor, Ferice) and a broader spread can be seen. Interestingly, Cloșani Cave had a wider spread in terms of both AWCD and richness with a positive trend, but mostly extended to the highest AWCD values (1.0 – 1.5) and maximum richness (close to 30). Also, a few samples from Ferice Cave also showed a positive trend, but this site actually depicted an intermediate metabolic activity and metabolic diversity richness. The widest range of richness and AWCD values have been counted for sediment, followed by water samples (Figure S4) the latter encountering the highest richness values. On the opposite, the moonmilk samples showed the lowest richness (< 10) and metabolic activity (< 0.1).

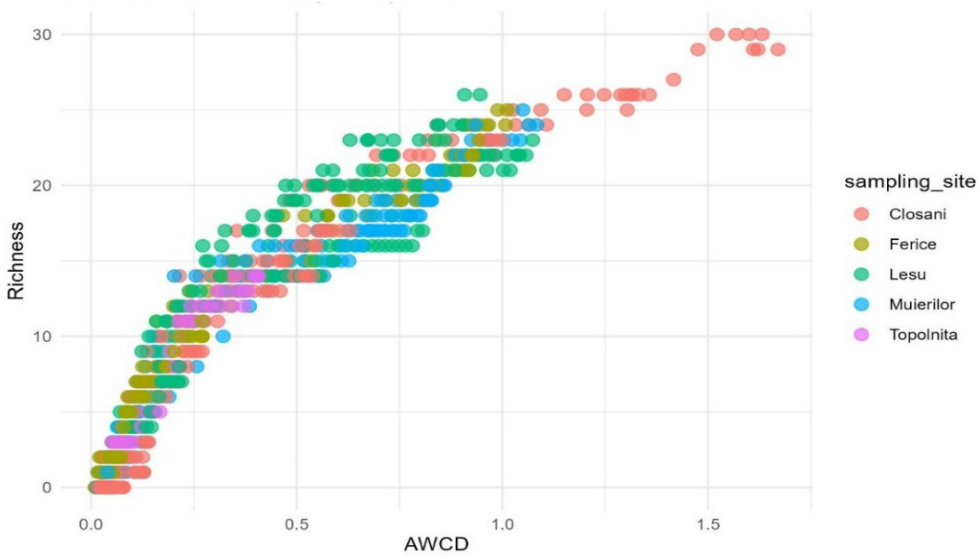

Figure 6. The scatter plot of AWCD and richness values measured at different time points over a total duration of 0-204 hours for all samples and sampling site.

Correlations between microbial metrics and chemistry

Correlation analysis identified key relationships between microbial activity metrics and environmental chemistry. AWCD correlated significantly with sodium ($r = 0.56$, $p < 0.01$) and phosphorus ($r = 0.45$, $p < 0.05$), while Shannon diversity correlated with electrical conductivity - EC ($r = 0.49$, $p < 0.05$) and magnesium ($r = 0.55$, $p < 0.05$). These results suggest that Na and P are positively associated with overall carbon substrate utilization rates (as indicated by AWCD), while EC, Na, and Mg contribute to shaping substrate preference patterns across microbial communities, as seen in the multivariate PCA analysis (Table 6, Figure 8).

Table 6. Pearson correlation coefficients for microbial activity metrics and environmental chemistry parameters. A single asterisk (*) denotes significance at the $p < 0.05$ level, and a double asterisk (**) denotes significance at the $p < 0.01$ level.

Metric	Na	P	EC	Mg	K
AWCD	0.56**	0.45*	0.39	0.55*	0.37
Richness	0.44*	0.32	0.48*	0.49*	0.30
Shannon Diversity	0.50*	0.40	0.49*	0.55*	0.41*

Analysis of microbial activity and carbon utilization in cave sediments

To assess microbial metabolic diversity across cave samples, hierarchical clustering and heatmaps were generated (Figure 7). These analyses revealed distinct metabolic profiles among sediment, water, and moonmilk samples.

Hierarchical AWCD clustering identified four microbial activity clusters (Supplementary Figure S5). Sediment samples from Cloşani and Muierilor caves showed consistently lower AWCD values, while water samples (e.g., PCDF2-APA, PLDF1B-APA) formed separate clusters with higher values, indicating greater microbial activity. Moonmilk samples (e.g., PFDF2MM and PFDFMMC) clustered with sediments, suggesting similar metabolic constraints. Similarly, substrate richness clustering highlighted high diversity in water samples (e.g. PCDF2-APA, PMDF9-APA, and PMDF10-APA) especially at later time points (116–204 hours), while samples like PFDF1 and PFDFMMC exhibited persistently low richness. High diversity was observed in GHICA2, PCDF2-APA, PMDF9-APA, and PMDF10-APA, whereas PFDF2, GHICA1, and PLDF3-APA displayed lower metabolic diversity, reflecting reduced microbial evenness.

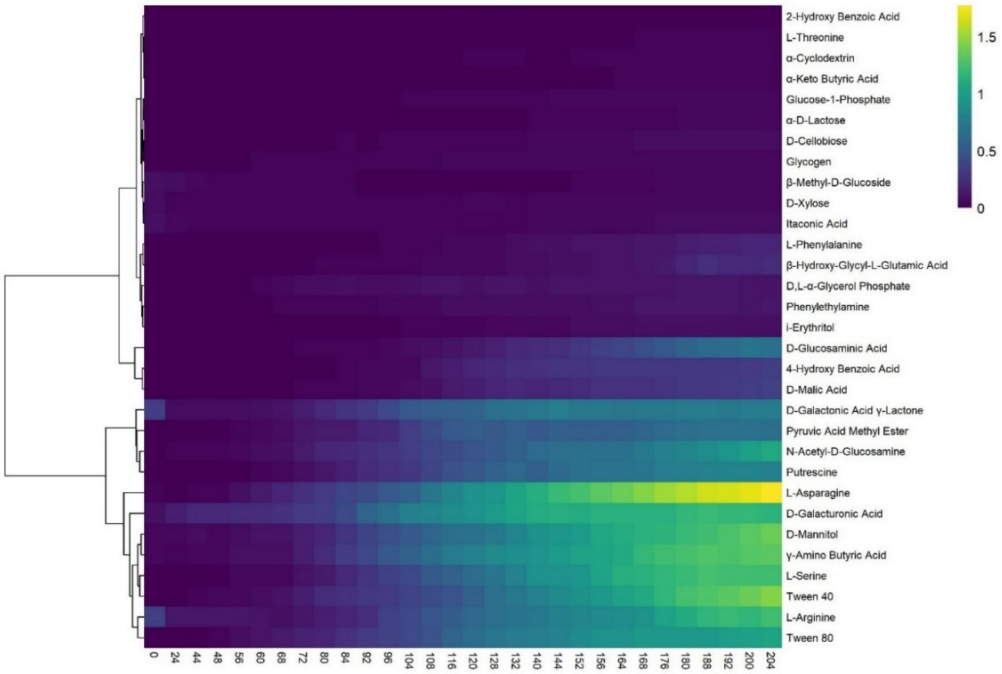

Figure 7. Heatmap plot of the median absorbance of microbial metabolic diversity across the carbon source types over time. The color scale represents absorbance values, with yellow indicating higher metabolic activity and purple indicating lower activity. Hierarchical clustering was applied to both carbon sources (rows) and time points (columns), revealing patterns of substrate utilization by the microbial communities over time.

Hierarchical clustering analysis was performed to examine microbial activity patterns based on carbon source utilization over time (Figure S7). Key findings indicated that L-asparagine and D-galacturonic acid show the highest metabolic activity after 120 hours (Figure S7). Noteworthy, Tween 40 and Tween 80 displayed increasing absorbance between 80 and 204 hours, suggesting delayed metabolism, likely due to shifts in microbial community structure or composition (Figure S7). Other carbon sources, including L-threonine, α-cyclodextrin, and α-keto butyric acid, exhibit minimal metabolic activity throughout the entire time period.

L-asparagine, Tween 80, and D-galacturonic acid were widely utilized across most of the samples, while L-threonine and α-keto butyric acid showed minimal microbial metabolization. Samples of sediment and moonmilk exhibit diminished overall metabolic activity, with the majority of carbon sources presenting low absorbance values, indicating a more restricted range of substrate use relative to water.

Environmental drivers of carbon substrate utilization

PCA was employed to examine the relationships between microbial metrics, including richness, Shannon diversity, and evenness along with several physico-chemical variables such as pH, EC, N, C, Na, Mg, K, Ca, and P. The first two components (PC1 and PC2) explained a significant proportion (>53%) of the data variation. The third component (PC3) gave an additional 10.9%, resulting in a cumulative explained variance of 64.6%. Water samples were strongly associated with higher microbial activity and substrate utilization diversity metrics (AWCD, richness, and Shannon diversity), driven primarily by EC. In contrast, sediment and moonmilk exhibited weak associations with all variables. An inverse correlation of Na and K with richness and AWCD suggests that increased concentrations of these ions may inhibit microbial activity and substrate utilization diversity (Figure 8).

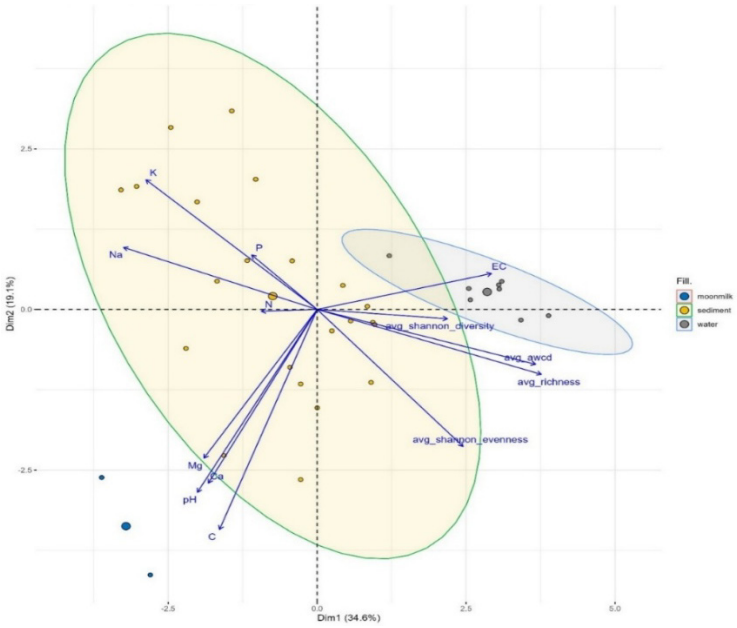

Figure 8. Principal Component Analysis (PCA) biplot showing the relationships between microbial metrics and cave chemistry variables across sample types. The first two principal components explain 34.6% and 19.1% of the variance, respectively. Microbial metrics such as average richness and AWCD are positively associated with EC, while pH, Ca, and Mg are negatively associated with microbial diversity metrics. The grouping of samples highlights distinct clustering based on sample type, with water samples clustering along higher EC values and sediment samples more spread out based on nutrient concentrations (Na, P, N, K).

Generalized Additive Models (GAMs) analysis

To capture complex, non-linear relationships between environmental variables and diversity metrics that usually evade the simpler PCA, GAMs have been employed to improve the accuracy of ecological predictions. The GAMs revealed that richness (Figure 9) and Shannon diversity (Figure 10) are strongly influenced by chemical variables, explaining 89.1% (first model) and 91.2% (second model) of the deviance. Richness showed nonlinear relationships with pH, K, and P ($p < 0.05$), while N and C had significant linear effects. Shannon diversity was significantly influenced by the nonlinear effects of EC and K ($p < 0.005$), while phophorus (P) was showing an exploratory trend toward significance ($p = 0.077$). A minor negative correlation was noticed between pH and Shannon diversity, suggesting that more basic environments may result in a slight decrease in diversity of consumed substrates (Figures 9 and 10).

Electrical conductivity (EC) emerged as a key factor influencing Shannon diversity (microbial substrate consumption diversity), showing a distinct nonlinear relationship (Figure 10). Shannon diversity peaked at intermediate EC levels (100–150 μS/cm) but declined at both lower and higher extremes. This aligns with the idea that intermediate ionic strength supports microbial functional diversity by optimizing nutrient transport without imposing osmotic stress. This suggests that EC below 100 may enhance substrate preference diversity, while fluctuations at higher levels (120–200) could have a negative impact. However, EC did not significantly affect Shannon evenness, suggesting its influence is more pronounced in shaping functional diversity in terms of microbial carbon substrate utilization rather than the uniformity of substrate preferences across the microbial community.

Phosphorus (P) had a strong negative effect on richness and evenness, but its relationship with Shannon diversity was non-linear, which peaked at intermediate P levels before declining at higher concentrations, suggesting that phosphorus may support certain taxa while reducing overall richness and evenness (Figures 9 and 10). The impact of chemical variables on Shannon evenness was investigated (Figure 11). The adjusted R^2 was 0.87, with 94.4% of the deviance explained. For example, variables such as sodium (Na) and magnesium (Mg), showed weak effects on richness (Figure 9) and Shannon diversity (Figure 10). However, Na displayed a non-linear relationship with Shannon evenness (Figure 11), suggesting that concentrations around 100 mg/kg may support a more even distribution of microbial substrate utilization preference, while extreme levels (<50 mg/kg or >200 mg/kg) could lead to disruption of evenness. Magnesium (Mg) did not show a strong effect on evenness (Figure 11). Potassium (K) had a strong negative effect on richness,

showing with increasing K levels (Figure 11), while with Shannon diversity it showed a non-linear relationship, peaking at intermediate levels before declining (Figure 10), suggesting that excessive K levels might reduce microbial metabolic C-utilization preferences. Lastly, calcium (Ca) was positively correlated with evenness (Figure 11), suggesting that elevated levels might promote a more even distribution of substrate utilization preference, whereas carbon (C) exhibited a slight decline with Shannon evenness, suggesting that higher concentrations might affect the distribution negatively.

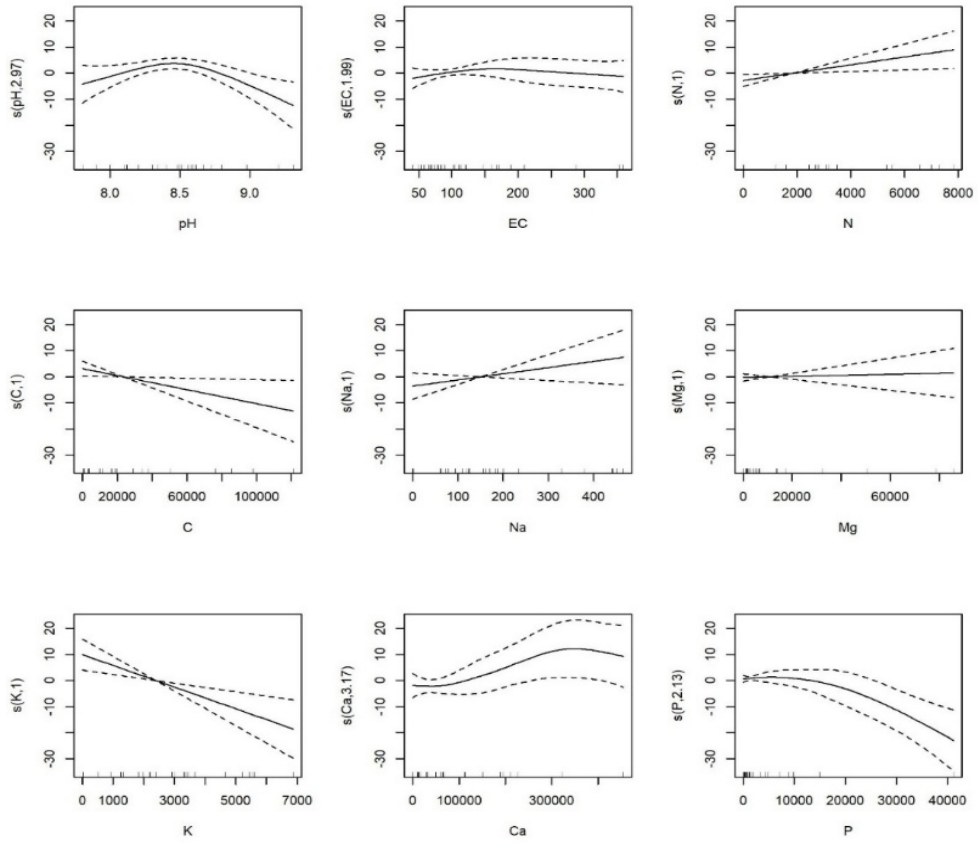

Figure 9. Generalized Additive Model plots showing the relationship between average richness and chemical factors (pH, EC, N, C, Na, Mg, K, Ca and P) in the analyzed cave samples. The solid lines represent the fitted smooths for each variable, while the dashed lines indicate the 95% confidence intervals. Variables with statistically significant relationships ($p < 0.05$) include pH, K, and P; variables with non-significant or marginal effects are included for completeness.

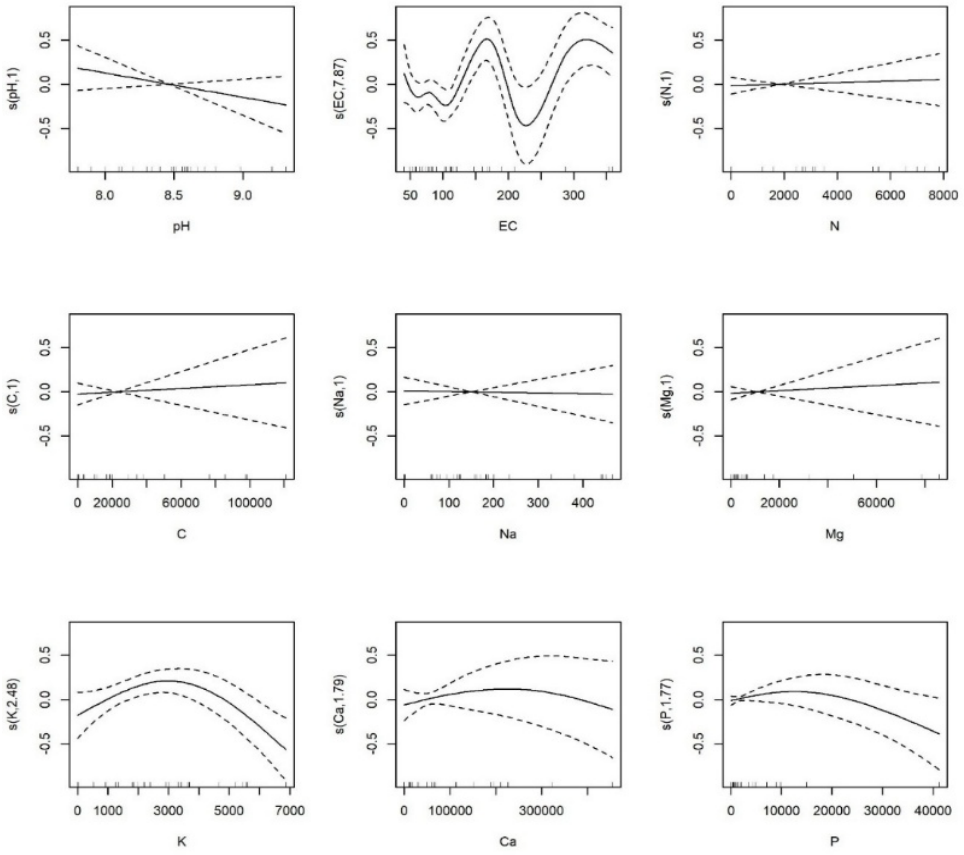

Figure 10. GAM plots showing the links between Shannon diversity and chemical factors (pH, EC, N, C, Na, Mg, K, Ca, and P). Solid lines represent the fitted smooths for each variable, while dashed lines indicate the 95% confidence intervals. Statistically significant relationships ($p < 0.05$) were found for EC and K; phosphorus (P) exhibited an exploratory trend toward significance ($p \approx 0.077$), while the other variables were not significant.

Besides sodium (Na), potassium (K) and carbon (C) which exhibited negative trends with evenness, EC, pH and N did not significantly influence evenness (Figure 11), suggesting that while some chemical variables might drive shifts in the distribution of microbial substrate utilization patterns, others have a more direct role in shaping the overall functional diversity.

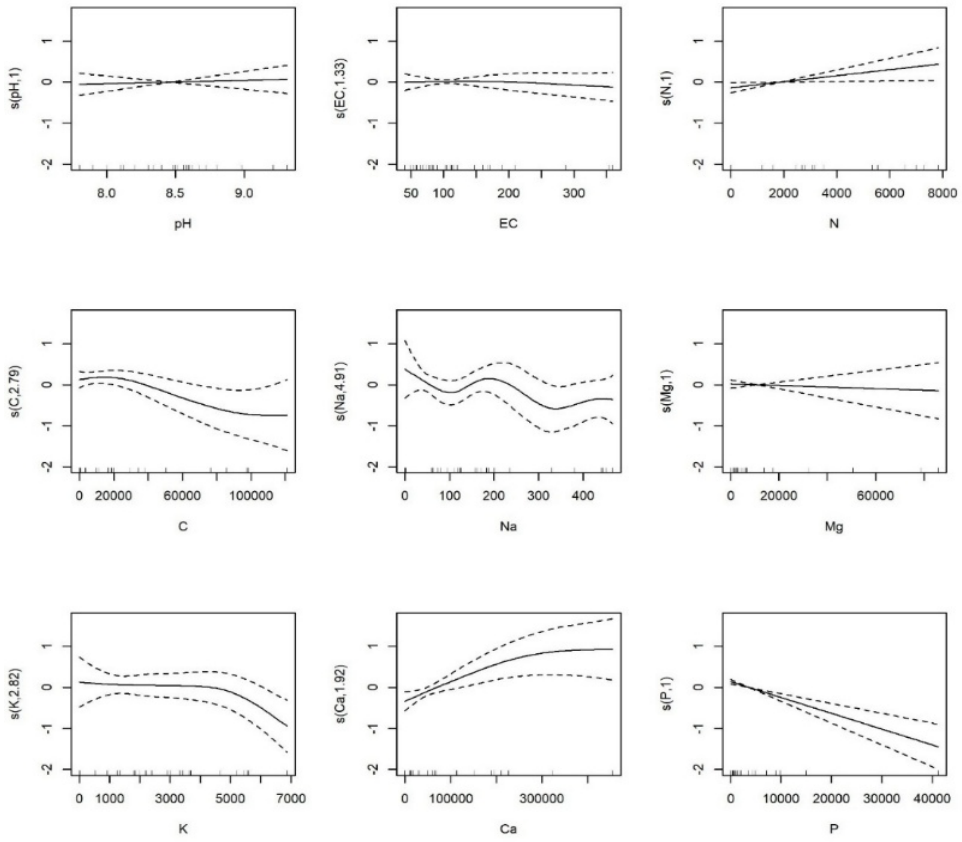

Figure 11. GAM plots of average Shannon evenness and different chemical factors (pH, EC, N, C, Na, Mg, K, Ca, and P). Solid lines represent the fitted smooths for each variable, while dashed lines indicate the 95% confidence intervals. No statistically significant relationships ($p < 0.05$) were observed; variables are shown for exploratory purposes.

Discussion

Variability and constraints in the analysis of carbon substrates utilization

After 200 hours of incubation, the C-substrate degradation patterns differed across water, sediment and moonmilk samples from Cloşani, Ferice, Muierilor, Leşu and Topolniţa caves. Although the same volume of inoculum was applied to

each well, we must take into consideration that there might be a variability in microbial inoculum size which may introduce inconsistencies in the results. Variability in microbial inoculum size likely contributed to discrepancies in optical density values, as showed by variations in wells containing the same substrate (Figure S1). Water samples showed greater C-substrate utilization potential and thus in microbial activity compared to sediment and moonmilk samples, supporting previous studies indicating that aquatic environments rich in organic matter support metabolically diverse communities (Obusan, 2023; Tobias-Hünefeldt *et al.*, 2023). Aquatic microbial communities are shaped by dynamic factors, including temperature and availability of organic carbon, which enhance their metabolic capabilities (Zheng *et al.*, 2014; Li *et al.*, 2021), suggesting that water environments can support a broader range of microbial taxa that can utilize diverse carbon sources. Thus, we could reasonably speculate on the relevance of aquatic microbial communities as key contributors to cave organic carbon degradation. Conversely, the stability of sediment and moonmilk geochemistry may restrain microbial diversity and its derived activity, with moonmilk samples displaying certain organic substrate degrading versatility. To the best of our knowledge, the present study is the first to evaluate the organic substrate utilization in moonmilk based on Biolog®EcoPlate™ approach and the few investigations on the metabolic potential of microorganisms associated with moonmilk formations prevent us from further assumptions.

The measurement of optical density in the Biolog®EcoPlate™ involves repeated handling and exposure to external environments, which increases the risk of contamination, especially for the plates incubated at temperatures higher than the room temperature (e.g., 37°C). Incubation was performed at 16°C to mitigate contamination risks and mimic cave conditions. Lower temperatures maintain microbial community structure while potentially decreasing metabolic activity, thereby improving the reliability of experimental outcomes (Akbari and Ghoshal, 2015; Tang *et al.*, 2017; Adekanmbi *et al.*, 2022).

Diversity analysis based on organic substrate metabolization

Despite the individual sample variation there are more metabolically active communities associated with higher microbial metabolic richness (Figure 5). Substrate utilization patterns varied by sample type, indicating variations in nutrient availability and environmental conditions. Sediment and water samples demonstrated greater microbial community-based substrate utilization diversity, whereas moonmilk associated microbial communities displayed intermediate richness. The findings correspond with research that associates substrate richness with improved metabolic functionality across various environmental conditions (Li *et al.*, 2017; Patsch *et al.*, 2018; Zhang *et al.*, 2020).

Hierarchical clustering and temporal analysis of substrate utilization showed distinct differentiation among sample types with distinct patterns across water, sediment, and moonmilk samples. Sediment samples demonstrated significant microbial metabolic versatility, employing various carbon sources as a result of the community heterogeneous composition (Meyer *et al.*, 2022). D-galacturonic acid, a major constituent of of pectin, is preferentially metabolized by microorganisms that colonize plant-associated environments. For instance, studies in Antarctic soils have revealed that the capacity to utilize D-galacturonic acid contributes to the metabolic diversity of resident microbiota, underscoring its ecological relevance in nutrient-poor and extreme environments (Pop *et al.*, 2025). Also, *Agrobacterium tumefaciens* have been demonstrated to possess dehydrogenases specific for D-galacturonic acid, facilitating its oxidation and subsequent use in central meteabolic pathways (Boer *et al.*, 2009; Parkkinen *et al.*, 2011). Here, sediment samples showed moderate C-substrate utilization with clear preferences for L-serine and L-arginine, but compared to water samples indicated a much lower metabolic efficiency. Koner *et al.* (2021) evaluated carbon substrate use patterns in limestone caves, demonstrating that microbial communities in sediment samples exhibited diverse metabolic activity. Their findings indicate that nutrient availability affects microbial growth, with sediment samples demonstrating greater richness and diversity than water samples, which contained more specialized communities. The clustering pattern of water samples exhibited selective carbon utilization, likely influenced by nutrient-rich yet special conditions (Pašić *et al.*, 2010; Power *et al.*, 2018; Tobias-Hünefeldt *et al.*, 2021). Additionally, members of the Fusobacteria have shown differential utilization of amino acids. Specifically, *Fusobacterium varium* has been reported to metabolize L-arginine, a capacity that distinguishes it from closely related species such as *Fusobacterium nucleatum*, which exhibit alternative substrate specificities (Ramezani *et al.*, 1999).

The microbial communities from moonmilk samples exhibited distinct substrate utilization patterns, especially for amino acids and amides, probably influenced by geological conditions such as high calcium carbonate content, low organic matter availabitlity, and stable microclimatic conditions chracateristic of moonmilk deposits (Nyyssönen *et al.*, 2014).

The broad range of metabolic activity inferred to Cloşani and Muierilor caves sediments underscores their microbial diversity and metabolic potential, aligning with findings from aquifer microbiome research (Wu *et al.*, 2015). Again, the separation of moonmilk samples in the dendrogram suggests that their distinct chemistry and environmental conditions support a specialized microbial community. Zheng and Gong (2019) and Theodorescu *et al.* (2023) evaluated niche differentiation within microbial communities and discovered that varying

environmental conditions can result in differences in microbial diversity and composition. Their findings support the idea that microbial communities within the moonmilk samples may have distinct metabolic requirements shaped by their environmental settings.

Moreover, it is important to consider that the findings of this study provide valuable insight into the functional potential of microbial communities but represent a temporal snapshot from a single season, spring. Despite the relative temperature of the caves it might be of interest to capture seasonal variations in microbial metabolic dynamics. Additionally, the set of carbon sources of Biolog® EcoPlates™ may not fully encompass the range of substrates utilized by the microbial communities, limiting insights into specific metabolic pathways or microbial identities. Future research combining metagenomics and broader substrate profiling could offer a more comprehensive understanding of the ecological roles of these communities.

Influence of environmental chemistry on C-substrate utilization capability

The Principal Component Analysis (PCA) illustrates clustering based on sample type, associating water samples with microbial metabolic diversity metrics (Shannon diversity, evenness, richness) and electrical conductivity, whereas sediment samples showed correlation with nutrient gradients, including potassium (K), phosphorus (P), and nitrogen (N). Moonmilk samples exhibited decreased associations, indicating unique microbial responses. The findings correspond with research emphasizing the impact of dissolved ions and nutrient gradients on microbial community structure and metabolic activity (Shaw *et al.*, 2008; Haegeman *et al.*, 2013; Park *et al.*, 2020).

Nutrient availability facilitated microbial growth in sediments, whereas elevated sodium concentrations were inhibitory, aligning with findings from cave and reservoir systems (Mandal *et al.*, 2017; D'Angeli *et al.*, 2019). Electrical conductivity influenced microbial metrics in water, influencing both diversity and activity (Shen *et al.*, 2022).

Generalized Additive Models (GAMs) further illustrated both linear (e.g., N, Na) and non-linear (e.g., K, P, Ca) influences of chemical variables on microbial metabolic diversity indices. Additionally, pH and electrical conductivity also showed non-linear effects. This underscores the significant impact of chemical environments on richness and metabolic potential of the microbial communities, similar to the study of Liu *et al.* (2023) in which GAMs were employed to examine the impact of different environmental variables on communities inhabiting the macrobenthos near Xiaoqing Estuary (Laizhou Bay, China) and their findings indicated that chemical factors, including salinity, organic matter, and nutrient

concentrations, significantly impacted biodiversity indices that are presumably linked to the metabolic activity, revealing both linear and non-linear relationships. Moreover, the study of the phytoplankton community structure in Lake Longhu (Jiang *et al.*, 2023) and the study of spatial patterns of biodiversity in a large marine ecosystem (Dencker *et al.*, 2017) revealed that environmental factors, including nutrient concentrations, had significant effects on the community variability.

Conclusions

In this study, we assessed the microbial metabolic diversity in cave sediment, water, and moonmilk samples using the Biolog® EcoPlate™ method, which enables rapid screening of carbon substrate utilization. Hierarchical clustering revealed significant differences between sample groups, with distinct functional profiles based on the sample's origin and geochemistry. Notably, this study is the first to apply Biolog® EcoPlates™ to moonmilk samples from karstic caves, highlighting the significance of employing novel approaches to explore the metabolic potential of microbial communities in cave environments.

The results revealed that microbial communities populating the cave water samples were the most metabolically versatile, utilizing a broad range of carbon substrates compared to those in sediment and moonmilk samples. D-galacturonic acid, L-asparagine, and Tween 80 were the most readily degraded C-substrates. Cave water hosted the most metabolically diverse microbial communities, playing a critical role in carbon turnover in studied cave systems, suggesting an important role in priming organic matter and facilitating nutrient cycling within the aquatic compartments of the caves. Sediment-associated communities exhibited more restricted metabolic profiles, favoring specific substrates like L-serine and L-arginine, reflecting potential specialization for recycling available organic substrates under more stable geochemical conditions. In contrast, moonmilk samples showed the least metabolic activity, with a narrow substrate range, indicating a specialized microbial community. Additionally, the application of Generalized Additive Models (GAMs) in cave microbiology is novel, providing a powerful approach for analyzing complex relationships between microbial metabolic diversity and environmental factors. GAMs revealed a positive correlation between Shannon diversity and intermediate values of electrical conductivity, indicating that moderate EC levels enhance microbial C-utilization.

Overall, this work offers fresh insights into the metabolic capacities of cave microbial communities and their adaptation to environmental variables, shedding light on their ecological significance in carbon cycling in cave environments. The observed patterns suggest that microbial communities might play key roles in carbon cycling in these subterranean karst ecosystems.

Acknowledgements and funding: This work was supported by a grant of the Ministry of Research, Innovation and Digitization, CNCS/CCCDI – UEFISCDI, project number 2/2019 (DARKFOOD), within PNCDI III. DFP has received financial support through the project: Entrepreneurship for innovation through doctoral and postdoctoral research, POCU/380/6/13/123886 co-financed by the European Social Fund, through the Operational Program for Human Capital 2014-2020. We thank to Ruxandra Bucur, Cristian Sitar, Alexandru Petculescu, Ionuț Cornel Mirea and Răzvan Arghir for their contribution to sampling campaigns.

Conflict of interest: The authors declare that the research was conducted in the absence of any commercial or financial relationships that could be construed as a potential conflict of interest.

Author contributions: DFP, HLB, OTM designed the research and drafted the manuscript; DFP and AC conducted the research; AMP performed the statistical analyses; OTM performed the sampling; EAL performed the chemical analyses. All authors contributed, verified, and approved the contents of the manuscript.

References

Adekanmbi, A. A., Shu, X., Zou, Y. & Sizmur, T. (2022). Legacy effect of constant and diurnally oscillating temperatures on soil respiration & microbial community structure. *Eur J Soil Sci.* 73(6), e13319, https://doi.org/10.1111/ejss.13319

Akbari, A., & Ghoshal, S. (2015). Effects of diurnal temperature variation on microbial community & petroleum hydrocarbon biodegradation in contaminated soils from a sub-Arctic site. Env. Micro., 17(12), 4916-4928, https://doi.org/10.1111/1462-2920.12846

Amaresan, N., Kumar, K., Venkadesaperumal, G., & Srivathsa, N. C. (2018). Microbial community level physiological profiles of active mud volcano soils in &aman & Nicobar Islands. *Nat. Acad. Sci. Lett.*, 41, 161-164, https://doi.org/10.25083/rbl/25.4/1731.1736

Asif, A., Koner, S., Chen, J. S., Hussain, A., Huang, S. W., Hussain, B., & Hsu, B. M. (2024). Uncovering the microbial community structure & physiological profiles of terrestrial mud volcanoes: a comprehensive metagenomic insight towards their Trichloroethylene biodegradation potentiality. *Env. Res.*, 119457, https://doi.org/10.1016/j.envres.2024.119457

Barton, H. A., and Northup, D. E. (2007). Geomicrobiology in cave environments: past, current and future perspectives. *J. Cave Karst Stud*., 69(1), 163-178.

Barton, H. A., Giarrizzo, J. G., Suarez, P., Robertson, C. E., Broering, M. J., Banks, E. D., & Venkateswaran, K. (2014). Microbial diversity in a Venezuelan orthoquartzite cave is dominated by the *Chloroflexi* (Class Ktedonobacterales) and *Thaumarchaeota* Group I. 1c. *Front. Microbiol*., 5, 615, https://doi.org/10.3389/fmicb.2014.00615

Bleahu, M., Decu, V., Negrea, S., Pleşa, C., Povară, I., &Viehmann, I. (1976). Caves from Romania. Editura Ştiinţifică şi Enciclopedică, Bucharest.

Boer, H., Maaheimo, H., Koivula, A., Penttilä, M., &Richard, P. (2009). Identification in *Agrobacterium tumefaciens* of the D-galacturonic acid dehydrogenase gene. *App. Microbio. Biotech*., 86(3), 901-909. https://doi.org/10.1007/s00253-009-2333-9

Bogdan D.F., Baricz A.I., Chiciudean I., Bulzu P.A., Cristea A., Năstase-Bucur R., Levei E.A., Cadar O., Sitar C., Banciu H.L. & Moldovan O.T., (2023), Diversity, distribution and organic substrates preferences of microbial communities of a low anthropic activity cave in North-Western Romania. *Front. Microbiol*. 14:962452, https://doi.org/10.3389/fmicb.2023.962452

Boteva, S., Stanachkova, M., Traykov, I., Angelova, B., & Kenarova, A. (2024). Bacterial functional responses to environmental variability: a case study in three distinct mountain lakes within a single watershed. *Biotechnol. Biotechnol. Equip*., 38(1), 2418549, https://doi.org/10.1080/13102818.2024.2418549

Bücs, S. L., Jére, C., Csősz, I., Barti, L., &Szodoray-Parády, F. (2012). Distribution and conservation status of cave-dwelling bats in the Romanian Western Carpathians. Vespertilio 16, 97–113.

Cacchio, P., &Del Gallo, M. (2019). A novel approach to isolation and screening of calcifying bacteria for biotechnological applications. *Geosci*., 9(11), 479, https://doi.org/10.3390/geosciences9110479

Cristea, A., Andrei, A. Ş., Baricz, A., Muntean, V., Banciu, H. L. (2014): Rapid assessment of carbon substrate utilization in the epilimnion of meromictic Ursu Lake (Sovata, Romania) by the Biolog Eco Plate™ approach. *Stud. Univ. Babes-Bolyai, Biol*. 59(1): 41-53

D'Angeli, I. M., Ghezzi, D., Leuko, S., Firrincieli, A., Parise, M., Fiorucci, A., & Cappelletti, M. (2019). Geomicrobiology of a seawater-influenced active sulfuric acid cave. *PLoS One*, 14(8), e0220706, https://doi.org/10.1371/journal.pone.0220706.

De Mandal, S., Chatterjee, R., &Kumar, N. S. (2017). Dominant bacterial phyla in caves and their predicted functional roles in C and N cycle. *BMC Microbio*., 17:90. https://doi.org/10.1186/s12866-017-1002-x

Dencker, T. S., Pecuchet, L., Beukhof, E., Richardson, K., Payne, M. R., & Lindegren, M. (2017). Temporal and spatial differences between taxonomic and trait biodiversity in a large marine ecosystem: Causes and consequences. *PLoS One*, 12(12), e0189731, https://doi.org/10.1371/journal.pone.0189731

Epure, L., Meleg, I. N., Munteanu, C. M., Roban, R. D., & Moldovan, O. T. (2014). Bacterial and fungal diversity of quaternary cave sediment deposits. *Geomicrobio. J*. 31, 116–127, https://doi.org/10.1080/01490451.2013.815292

Feigl, V., Ujaczki, É., Vaszita, E., &Molnár, M. (2017). Influence of red mud on soil microbial communities: Application and comprehensive evaluation of the Biolog® EcoPlate™ approach as a tool in soil microbiological studies. *Sci. Tot. Env*., 595, 903-911, https://doi.org/10.1016/j.scitotenv.2017.03.266

Garland, J. L. (1997). Analysis and interpretation of community-level physiological profiles in microbial ecology. *FEMS Microbio. Eco.*, 24(4), 289-300, https://doi.org/10.1111/j.1574-6941.1997.tb00446.x

Ghaly, T. M., Focardi, A., Elbourne, L. D. H., *et al.* (2023). Stratified microbial communities in Australia's only anchialine cave are taxonomically novel and drive chemotrophic energy production via coupled nitrogen-sulphur cycling. *Microbiome*, 11, 190. https://doi.org/10.1186/s40168-023-01633-8

Gryta, A., Frąc, M., &Oszust, K. (2014). The application of the Biolog EcoPlate approach in ecotoxicological evaluation of dairy sewage sludge. Applied biochemistry and biotechnology, 174, 1434-1443, https://doi.org/10.1007/s12010-014-1131-8

Gryta, A., Frąc, M., &Oszust, K. (2014). The application of the Biolog EcoPlate approach in ecotoxicological evaluation of dairy sewage sludge. *App. Biochem. Biotech*., 174, 1434-1443, https://doi.org/10.1007/s12010-014-1131-8

Haegeman, B., Hamelin, J., Moriarty, J., Neal, P., Dushoff, J., &Weitz, J. S. (2013). Robust estimation of microbial diversity in theory and in practice. *The ISME journal*, 7(6), 1092-1101, https://doi.org.10.1038/ismej.2013.10

Inskeep, W. P., Jay, Z. J., Tringe, S. G., Herrgård, M. J., Rusch, D. B., &YNP Metagenome Project Steering Committee and Working Group Members. (2013). The YNP metagenome project: environmental parameters responsible for microbial distribution in the Yellowstone geothermal ecosystem. *Front. Microbiol*., 4, 67, https://doi.org. 10.3389/fmicb.2013.00067

Iţcuş, C., Pascu, M. D., Brad, T., Perşoiu, A., &Purcarea, C. (2016). Diversity of cultured bacteria from the perennial ice block of Scarisoara Ice Cave, Romania. *Int. J. Speleo*., 45(1), 9, http://dx.doi.org/10.5038/1827-806X.45.1.1948

Jałowiecki, Ł., Chojniak, J. M., Dorgeloh, E., Hegedusova, B., Ejhed, H., Magnér, J., &Płaza, G. A. (2016). Microbial community profiles in wastewaters from onsite wastewater treatment systems technology. *PloS one*, 11(1), e0147725, https://doi.org/10.1371/journal.pone.0147725

Jiang, Y., Wang, Y., Huang, Z., Zheng, B., Wen, Y., &Liu, G. (2023). Investigation of phytoplankton community structure and formation mechanism: a case study of Lake Longhu in Jinjiang. *Front. Microbiol*., 14, 1267299, https://doi.org.10.3389/fmicb.2023.1267299

Jin, Q., Black, A., Kales, S. N., Vattem, D., Ruiz-Canela, M., &Sotos-Prieto, M. (2019). Metabolomics and Microbiomes as Potential Tools to Evaluate the Effects of the Mediterranean Diet. *Nutrients*, 11(1), 207, https://doi.org/10.3390/nu11010207

Jones, D. (2015). 2. Methods for Characterizing Microbial Communities in Caves &Karst: A Review. In A. Summers Engel (Ed.), Microbial Life of Cave Systems (pp. 23-46). Berlin, München, Boston: De Gruyter, https://doi.org/10.1515/9783110339888-004

Koner, S., Chen, J. S., Hsu, B. M., Rathod, J., Huang, S. W., Chien, H. Y., ... &Chan, M. W. (2022). Depth-resolved microbial diversity and functional profiles of trichloroethylene-contaminated soils for Biolog EcoPlate-based biostimulation strategy. *J. Hazard. Mater.*, 424, 127266, https://doi.org/10.1016/j.jhazmat.2021.127266

Koner, S., Chen, J. S., Hsu, B. M., Tan, C. W., Fan, C. W., Chen, T. H., &Nagarajan, V. (2021). Assessment of Carbon substrate catabolism pattern and functional metabolic pathway for Microbiota of Limestone Caves. *Microorganisms*, 9, https://doi.org/10.3390/microorganisms9081789

Li, H., Xu, Z., Yan, Q., Yang, S., Van Nostrand, J. D., Wang, Z., &Deng, Y. (2018). Soil microbial beta-diversity is linked with compositional variation in aboveground plant biomass in a semi-arid grassland. *PLANTSOIL*, 423, 465-480, https://doi.org/10.1007/s11104-017-3524-2

Li, X., Liu, L., Zhu, Y., Zhu, T., Wu, X., &Yang, D. (2021). Microbial community structure and its driving environmental factors in black carp (Mylopharyngodon piceus) aquaculture pond. Water, 13(21), 3089, https://doi.org/10.3390/w13213089

Liu, F., Giometto, A., &Wu, M. (2021). Microfluidic and mathematical modeling of aquatic microbial communities. *Anal. Bioanal. Chem*., 413, 2331–2344, https://doi.org/10.1007/s00216-020-03085-7

Liu, L., Li, A., Zhu, L., Xue, S., Li, J., Zhang, C., &Mao, Y. (2023). The Application of the Generalized Additive Model to Represent Macrobenthos near Xiaoqing Estuary, Laizhou Bay. *Biology*, 12(8), 1146, https://doi.org/10.3390/biology12081146

Martin-Pozas, T., Gonzalez-Pimentel, J. L., Jurado, V., Cuezva, S., Dominguez-Moñino, I., Fernandez-Cortes, A., &Saiz-Jimenez, C. (2020). Microbial activity in subterranean ecosystems: Recent advances. *Appl. Sci.*, 10(22), 8130, https://doi.org/10.3390/app10228130

Melita, M., Amalfitano, S., Preziosi, E., Ghergo, S., Frollini, E., Parrone, D., &Zoppini, A. (2023). Redox conditions and a moderate anthropogenic impairment of groundwater quality reflected on the microbial functional traits in a volcanic aquifer. *Aquat. Sci*., 85(1), 3, https://doi.org/10.1007/s00027-022-00899-8

Meyer, N. R., Parada, A. E., Kapili, B. J., Fortney, J. L., &Dekas, A. E. (2022). Rates and physico-chemical drivers of microbial anabolic activity in deep-sea sediments and implications for deep time. *Environ. Microbiol.*, 24(11), 5188-5201, https://doi.org/10.1111/1462-2920.16183

Moldovan, O. T., Carrell, A. A., Bulzu, P. A., Levei, E., Bucur, R., Sitar, C., &Podar, M. (2023). The gut microbiome mediates adaptation to scarce food in Coleoptera. *Environ. Microbiol.*, 18(1), 80, https://doi.org/10.1186/s40793-023-00537-2

Moretti, G., Matteucci, F., Ercole, C., Vegliò, F., &Del Gallo, M. (2016). Microbial community distribution and genetic analysis in a sludge active treatment for a complex industrial wastewater: A study using microbiological and molecular analysis and principal component analysis. *Ann. Microbiol.*, 66, 397-405, https://doi.org/10.1007/s13213-015-1122-1

Morita, N., Toma, Y., &Ueno, H. (2024). Microbial diversity and community structure in co-composted bamboo powder and tea leaves based on carbon substrate utilization patterns of the BIOLOG EcoPlate method. *Adv. Bamboo Sci*., 8, 100101, https://doi.org/10.1016/j.bamboo.2024.100101

Musat, N., Musat, F., Weber, P. K., &Pett-Ridge, J. (2016). Tracking microbial interactions with NanoSIMS. *COBIOT*, 41, 114–121, https://doi.org/10.1016/j.copbio.2016.06.007

Nyyssönen, M., Hultman, J., Ahonen, L., Kukkonen, I., Paulin, L., Laine, P., &Auvinen, P. (2014). Taxonomically and functionally diverse microbial communities in deep crystalline rocks of the Fennoscandian shield. *The ISME journal*, 8(1), 126-138, https://doi.org/10.1038/ismej.2013.125

Obusan, M. C. M., Castro, A. E., Villanueva, R. M. D., Isagan, M. D. E., Caras, J. A. A., &Simbahan, J. F. (2023). Physico-Chemical Quality and Physiological Profiles of Microbial Communities in Freshwater Systems of Mega Manila, Philippines. *Data*, 8(6), 103, https://doi.org/10.3390/data8060103

O'Connor, B. R., Fernández-Martínez, M. Á., Léveillé, R. J., & Whyte, L. G. (2021). Taxonomic characterization and microbial activity determination of cold-adapted microbial communities in Lava Tube Ice Caves from Lava Beds National Monument, a high-fidelity Mars analogue environment. *Astrobio.*, 21(5), 613-627, https://doi.org/10.1089/ast.2020.2327

Park, S., Cho, Y. J., Jung, D. Y., Jo, K. N., Lee, E. J., &Lee, J. S. (2020). Microbial diversity in moonmilk of Baeg-nyong Cave, Korean CZO. Front. Microbiol., 11, 613, https://doi.org/10.3389/fmicb.2020.00613

Pašić, L., Kovče, B., Sket, B., and Herzog-Velikonja, B. (2009). Diversity of microbial communities colonizing the walls of a Karstic cave in Slovenia. *FEMS Microbio. Eco.*, 71(1), 50-60, https://doi.org/10.1111/j.1574-6941.2009.00789.x

Parkkinen, T., Boer, H., Jänis, J., Andberg, M., Penttilä, M., Koivula, A., & Rouvinen, J. (2011). Crystal structure of uronate dehydrogenase from *Agrobacterium tumefaciens*. *JBC*, 286(31), 27294-27300. https://doi.org/10.1074/jbc.m111.254854

Patsch, D., van Vliet, S., Marcantini, L. G., &Johnson, D. R. (2018). Generality of associations between biological richness and the rates of metabolic processes across microbial communities. *Environ. Microbiol.*, 20(12), 4356-4368, https://doi.org/10.1111/1462-2920.14352

Paula, C. C. P. D., Bichuette, M. E., &Seleghim, M. H. R. (2020). Nutrient availability in tropical caves influences the dynamics of microbial biomass. *MicrobiologyOpen*, 9(7), e1044, https://doi.org/10.1002/mbo3.1044

Pedersen, K. (2012). Subterranean microbial populations metabolize hydrogen and acetate under in situ conditions in granitic groundwater at 450 m depth in the Äspö Hard Rock Laboratory, Sweden. *FEMS Microbio. Eco*., 81(1), 217–229. https://doi.org/10.1111/j.1574-6941.2012.01370.x

Pop, C.-E., Fendrihan, S., Crăciun, N., Vasilighean, G., Chifor, D. E., Topârceanu, F., Florea, A., Mihăilescu, D. F., &Mernea, M. (2025). Antarctic Soil and Viable Microbiota After Long-Term Storage at Constant −20 °C. *Biology*, *14*(3), 222. https://doi.org/10.3390/biology14030222

Power, J. F., Carere, C. R., Lee, C. K., Wakerley, G. L., Evans, D. W., Button, M., &Stott, M. B. (2018). Microbial biogeography of 925 geothermal springs in New Zealand. *Nature communications,* 9(1), 2876, https://doi.org/10.1038/s41467-018-05020-y

Ramezani, M., MacIntosh, S., &White, R. L. (1999). Utilization of d-amino acids by *Fusobacterium nucleatum* and *Fusobacterium varium*. *Amino Acids*, 17(2), 185-193. https://doi.org/10.1007/bf01361881

Rutgers, M., Wouterse, M., Drost, S. M., Breure, A. M., Mulder, C., Stone, D., &Bloem, J. (2016). Monitoring soil bacteria with community-level physiological profiles using Biolog™ Ecoplates in the Netherlands and Europe. *Appl. Soil Ecol.*, 97, 23-35, https://doi.org/10.1016/j.apsoil.2015.06.007

Shaw, A. K., Halpern, A. L., Beeson, K., Tran, B., Venter, J. C., &Martiny, J. B. (2008). It's all relative: ranking the diversity of aquatic bacterial communities. *Environ. Microbiol*, 10(9), 2200-2210, https://doi.org.10.1111/j.1462-2920.2008.01626.x

Shen, J., Smith, A. C., Barnett, M. J., Morgan, A., & Wynn, P. M. (2022). Distinct microbial communities in the soils, waters, and speleothems of a hyperalkaline cave system. Journal of Geophysical Research: *Biogeosciences*, 127(9), e2022JG006866, https://doi.org/10.3390/microorganisms9081789

Simpson, G. L., (2024). gratia: An R package for exploring generalized additive models. *J Open Source Software*, 9(104), 6962, https://doi.org/10.21105/joss.06962

Sofo, A., & Ricciuti, P. (2019). A standardized method for estimating the functional diversity of soil bacterial community by Biolog® EcoPlatesTM assay—the case study of a sustainable olive orchard. *App. Sci.*, 9(19), 4035, https://doi.org/10.3390/app9194035

Stefanowicz, A. (2006). The Biolog plates technique as a tool in ecological studies of microbial communities. *Pol. J. Environ. Stud*., 15(5).

Tang, Z., Sun, X., Luo, Z., He, N., & Sun, O. J. (2018). Effects of temperature, soil substrate, and microbial community on carbon mineralization across three climatically contrasting forest sites. *Eco. Evo.*, 8(2), 879-891, https://doi.org/10.1002/ece3.3708

Teng, Z., Fan, W., Wang, H., Cao, X., & Xu, X. (2020). Monitoring soil microorganisms with community-level physiological profiles using Biolog EcoPlates™ in Chaohu lakeside wetland, East China. *Eurasian J. Soil Sci.*, 53, 1142-1153, https://doi.org/10.1134/S1064229320080141

Theodorescu, M., Bucur, R., Bulzu, PA., Faur L., Levei EA., Mirea IC, Cadar O., Ferreira R, Souza-Silva M., & Moldovan OT. (2023). Environmental Drivers of the Moonmilk Microbiome Diversity in Some Temperate and Tropical Caves. *Microb Ecol*, 86,2847-2857, https://doi.org/10.1007/s00248-023-02286-8

Thompson, H. F., & Gutierrez, T. (2021). Detection of hydrocarbon-degrading bacteria on deepwater corals of the northeast Atlantic using CARD-FISH. *J. Microbiol. Methods*., 187, 106277, https://doi.org/10.1016/j.mimet.2021.106277

Tobias-Hünefeldt, S. P., Wing, S. R., Baltar, F., & Morales, S. E. (2021). Changes in microbial community phylogeny and metabolic activity along the water column uncouple at near sediment aphotic layers in fjords. *Sci. Rep*., 11(1), 19303, https://doi.org/10.1038/s41598-021-98519-2

Wu, X., Holmfeldt, K., Hubalek, V., Lundin, D., Åström, M., Bertilsson, S., & Dopson, M. (2016). Microbial metagenomes from three aquifers in the Fennoscandian shield terrestrial deep biosphere reveal metabolic partitioning among populations. *The ISME Journal*, 10(5), 1192-1203, https://doi.org/10.1038/ismej.2015.185

Yu, K., Yi, S., Li, B., *et al.* (2019). An integrated meta-omics approach reveals substrates involved in synergistic interactions in a bisphenol A (BPA)-degrading microbial community. *Microbiome*, 7(1), 16. https://doi.org/10.1186/s40168-019-0634-5

Yu, Z., Yang, J., Amalfitano, S., Yu, X., & Liu, L. (2014). Effects of water stratification and mixing on microbial community structure in a subtropical deep reservoir. *Sci. Rep*., 4(1), 5821, https://doi.org/10.1038/srep05821

Yun, Y., Cheng, X., Wang, W., & Wang, H. (2018). Seasonal variation of bacterial community and their functional diversity in drip water from a karst cave. *Chinese Science Bulletin*, 63(36), 3932-3944, https://doi.org/10.1360/N972018-00627

Zak, J. C., Willig, M. R., Moorhead, D. L., & Wildman, H. G. (1994). Functional diversity of microbial communities: a quantitative approach. *Soil Biol. Biochem*., 26(9), 1101-1108, https://doi.org/10.1016/0038-0717(94)90131-7

Zhang, P., Cui, Z., Guo, M., & Xi, R. (2020). Characteristics of the soil microbial community in the forestland of Camellia oleifera. *Peer J* 8: e9117, https://doi.org.10.7717/peerj.9117

Zheng, Y., & Gong, X. (2019). Niche differentiation rather than biogeography shapes the diversity and composition of microbiome of Cycas panzhihuaensis. *Microbiome*, 7, 1-19, https://doi.org/10.1186/s40168-019-0770-y

Zoltan, L., & Szántó, L. (2003). Bats of the Carpathian Region. *Acta Chiropt*. 5, 155–160. https://doi.org/10.3161/001.005.0115

Supplementary materials

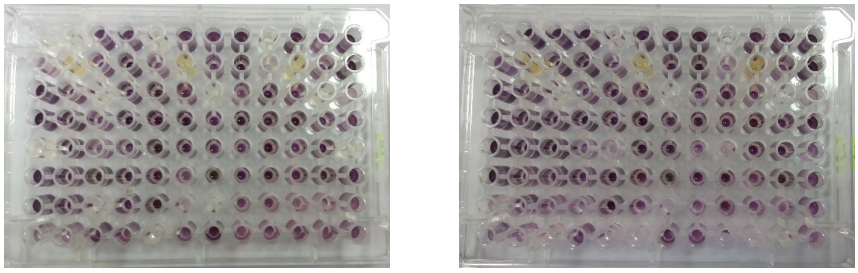

PCDF2-LIMON PCDF3-APA

Figure S1. Random selection of pictures showing the degradation patterns within Biolog® EcoPlates™ after an incubation period of 200 hours (PC – Closani Cave)

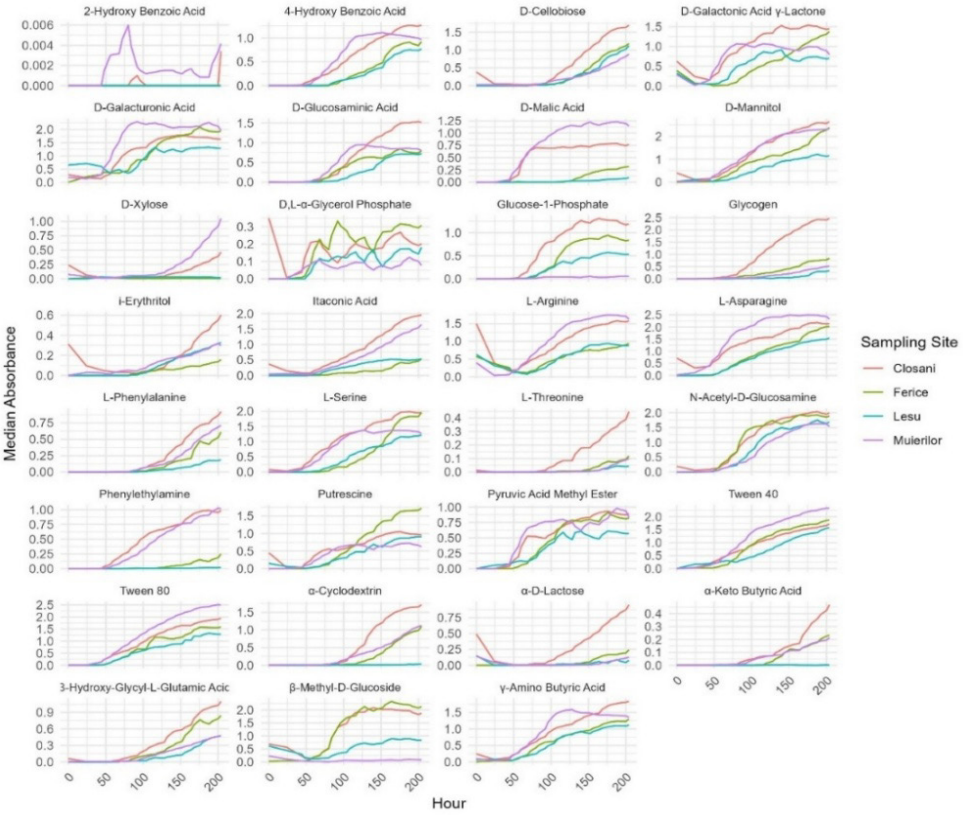

Figure S2. Median absorbance over time by carbon and sampling site for water samples only.

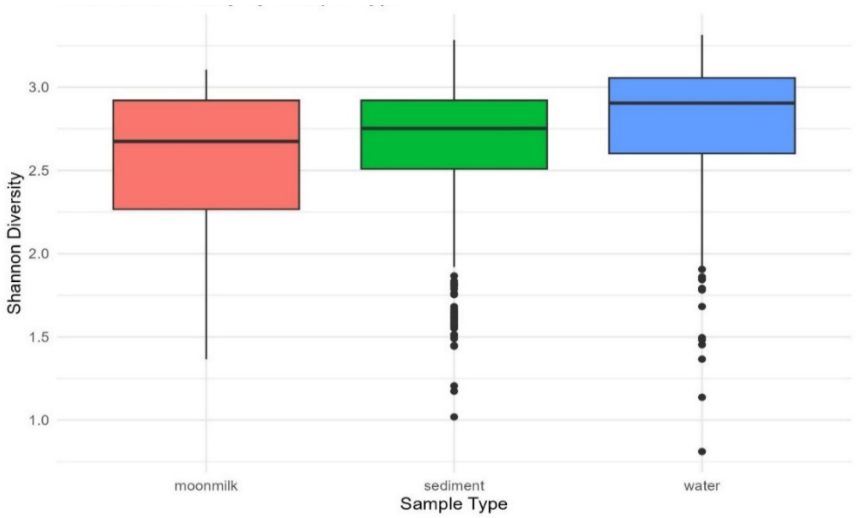

Figure S3. Shannon diversity (metabolic diversity) index of microbial communities in moonmilk, sediment, and water samples. Water samples show the highest diversity, followed by moonmilk and sediments. Boxplots display median, interquartile range, and outliers.

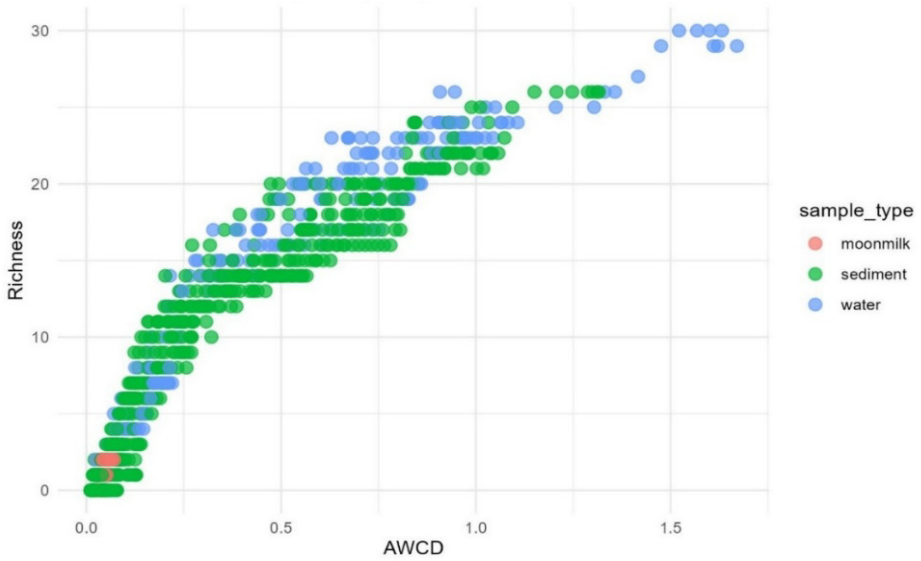

Figure S4. Scatter plot of AWCD versus richness of substrate degradation for sediments, moonmilk, and water samples, measured over time (0–204 hours).

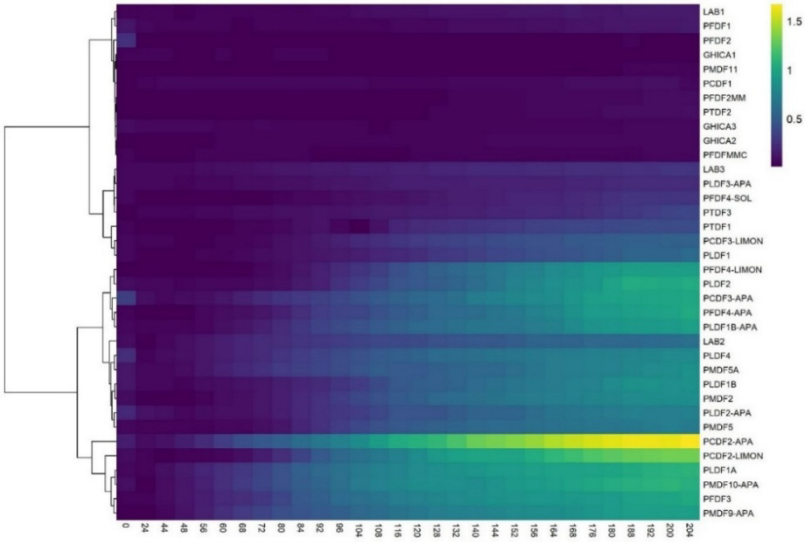

Figure S5. Heatmap of the average-well color development by sample and hour with clustering. See Table 1 for corresponding sample types and codes.

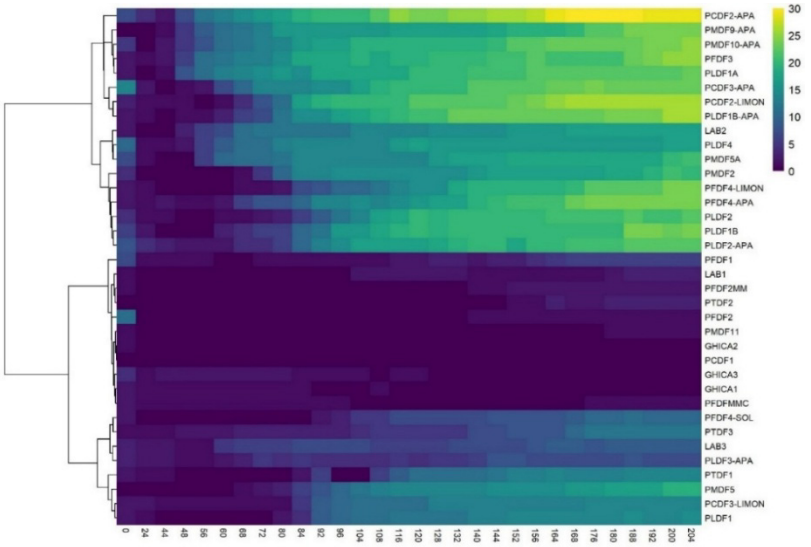

Figure S6. The heatmap showing the clustering of substrate richness by sample and hour. All the sample types are included in the analysis. The color scale represents species richness, with yellow indicating higher richness and dark purple representing lower richness. Hierarchical clustering was applied to both samples (rows) and time points (columns), revealing distinct temporal and sample-specific patterns in microbial diversity. See Table II.1 for corresponding sample types and codes.

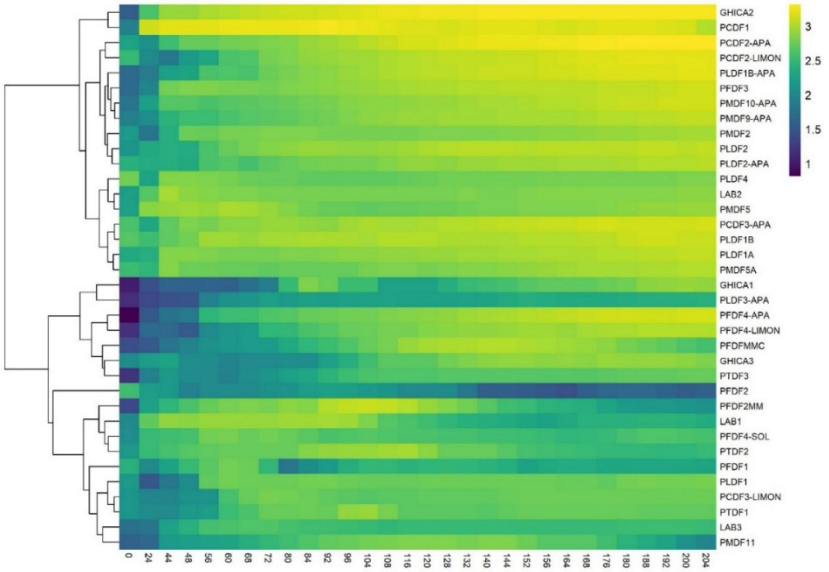

Figure S7. Dendrogram heatmap showing the clustering of Shannon diversity across different samples over time. The color scale represents Shannon diversity, with yellow indicating higher diversity and purple representing lower diversity. Hierarchical clustering was applied to both samples (rows) and time points (columns), revealing distinct temporal and sample-specific patterns in microbial diversity.

Table S1. Maximum AWCD values for water, sediment, and moonmilk samples across the sampling sites.

Site	Max AWCD (Water)	Max AWCD (Sediment)	Max AWCD (Moonmilk)
Cloșani	1.67	1.32	-
Ferice	1.01	1.01	0.07
Leșu	0.95	1.07	-
Muierilor	1.08	0.84	-
Topolnița	-	0.41	-

Table S2. List of geochemical parameters excluded from the PCA analysis, including elements (Al, Fe, S, Mn, As, Cr, Co, Ni, Cu, Zn) and water-specific parameters (DIC, DOC, SO_4^{2-}, NO_3^-, Cl^-, PO_4^{3-}), excluded for either low concentrations or incompatibility between sediment and water sample data.

Parameters																
	Al	**Fe**	**S**	**Mn**	**As**	**Cr**	**Co**	**Ni**	**Cu**	**Zn**	**DIC**	**DOC**	**SO_4^{2-}**	**NO_3^-**	**Cl^-**	**PO_4^{3-}**
sediments																
Sample ID	mg/kg	mg/kg	mg/kg	mg/kg	mg/kg	mg/kg	mg/kg	mg/kg	mg/kg	mg/kg	-	-	-	-	-	-
PMDF2	3903	4617	68.4	214	52.7	4.0	1.3	4.6	11.0	60.3	-	-	-	-	-	-
PMDF5	14847	27613	196	158	15.6	38.0	3.4	9.3	467	242	-	-	-	-	-	-
PMDF11	14370	14303	286	570	33.5	17.0	3.1	12.3	19.8	784	-	-	-	-	-	-
PMDF5A	16427	23567	322	195	8.2	6.0	1.8	6.4.0	35.1	56.0	-	-	-	-	-	-
PTDF1	24903	33967	92.7	586	6.1	66.0	12.7	29.3	22.6	83.3	-	-	-	-	-	-
PTDF2	25773	34367	37	635	5.5	59.0	12.9	28.2	21.0	64.6	-	-	-	-	-	-
PTDF3	14866	23100	206	81.2	5.3	8.5	1.7	5.0	3.4	9.2	-	-	-	-	-	-
LAB1	33362	30139	27.6	1097	5.1	49.7	19.7	51.7	51.2	156	-	-	-	-	-	-
LAB2	24540	22837	46.7	186	13.5	42.2	6.7	40.2	28.9	489	-	-	-	-	-	-
LAB3	38107	28104	39.6	138	11.9	34.0	5.2	32.5	21.5	153	-	-	-	-	-	-
GHICA1	62997	55572	61.1	313	13.9	93.7	8.2	69.7	46.4	148	-	-	-	-	-	-
GHICA2	63089	53824	85.8	305	14.1	89.7	8.2	72.8	47.1	154	-	-	-	-	-	-
GHICA3	57706	45181	47.3	304	13.1	89.0	8.1	73.1	49.6	156	-	-	-	-	-	-
PCDF1	27557	39667	30.9	945	6.2	44.0	14.1	30.0	32.7	96.5	-	-	-	-	-	-
PFDF1	28283	32257	59.0	622	20.2	38.0	7.7	27.0	15.8	130	-	-	-	-	-	-
PFDF2	25933	31157	31.8	998	17.2	38.0	10.6	31.5	17.1	111	-	-	-	-	-	-

Table S2 continued

Parameters																
	Al	**Fe**	**S**	**Mn**	**As**	**Cr**	**Co**	**Ni**	**Cu**	**Zn**	**DIC**	**DOC**	**SO_4^{2-}**	**NO_3^-**	**Cl^-**	**PO_4^{3-}**
PFDF3	40033	32097	67.8	686	19.7	46.0	11.0	23.9	17.6	170	-	-	-	-	-	-
PFDFMMC	12768	6089	24.5	128	29.6	13.4	1.8	17.6	1.6	31.3	-	-	-	-	-	-
PFDF2MM	3286	1853	86.2	66.3	5.6	5.6	1.2	6.0	0.3	14.7	-	-	-	-	-	-
PLDF1	9543	16157	36	411	23.8	13	5.5	13.9	5.5	28.5	-	-	-	-	-	-
PLDF1A	19853	26813	734	161	13.4	5	1.5	5.0	5.4	16.3	-	-	-	-	-	-
PLDF1B	18113	25193	176	832	53.3	21	8.3	27.8	26.0	134	-	-	-	-	-	-
PLDF4	12183	22273	128	745	51.0	19	7.3	25.1	28.5	134	-	-	-	-	-	-
PLDF2	18173	27787	801	272	13.8	4.7	1.8	5.9	8.7	51.4	-	-	-	-	-	-
water																
	µg/L	µg/L	-	µg/L	µg/L	µg/L	µg/L	µg/L	µg/L	µg/L	mg/L	mg/L	mg/L	mg/L	mg/L	mg/L
PMDF9-APA	<0.2	30.0	NA	0.20	0.50	1.00	<0.2	<0.2	0.7	5.1	16.9	3.3	13.5	61.5	1.9	13.5
PMDF10-APA	<0.2	30.0	NA	0.20	0.80	1.20	<0.2	0.4	0.9	3.5	19.8	2.1	28.0	78.5	2.7	28.0
PCDF2-APA	7.8	6800	NA	0.30	0.30	<0.2	<0.2	0.3	0.4	7.4	18.9	1.6	7.5	1.9	0.8	7.5
PCDF3-APA	<0.2	160	NA	0.40	<0.20	<0.2	<0.2	0.4	0.3	11.9	19.9	2.5	5.1	1.4	0.8	5.1
PFDF4-APA	<0.2	100	NA	0.70	0.70	<0.2	<0.2	<0.2	0.3	5.5	48.6	0.2	6.4	1.2	1.0	6.4
PLDF1B-APA	<0.2	10.0	NA	0.40	0.90	<0.2	<0.2	0.3	0.3	4.6	17.0	0.8	4.6	4.3	0.8	4.6
PLDF2-APA	<0.2	10.0	NA	0.30	1.40	<0.2	<0.2	<0.2	0.1	2.7	19.5	0.9	4.7	4.2	0.7	4.7
PLDF3-APA	<0.2	20.0	NA	0.30	0.70	1.50	<0.2	<0.2	0.3	10.2	24.2	1.0	7.7	2.3	0.7	7.7
PMDF9-APA	<0.2	30.0	NA	0.20	0.50	1.00	<0.2	<0.2	0.7	5.1	16.9	3.3	13.5	61.5	1.9	13.5